ELSEVIER

Catalysis Today 35 (1997) 339–365

CATALYSIS TODAY

Review

Titania-based aerogels

M. Schneider [1], A. Baiker *

Department of Chemical Engineering and Industrial Chemistry, Swiss Federal Institute of Technology, ETH-Zentrum, CH-8092 Zürich, Switzerland

Abstract

The potential of aerogels for catalysis resides in their unique morphological and chemical properties. These properties originate from their wet-chemical preparation via the sol-gel method and the subsequent removal of solvent by supercritical drying. The present state of supercritical drying can be divided into the high-temperature and low-temperature methods, usually based on alcoholic solvents and CO_2, respectively. First, the ceramic and catalytic use of unitary titania are considered, revealing the importance of titania in many respects. A survey of the salient literature about sol-gel chemistry, either itself or in conjunction with supercritical drying, and catalysis stresses the potential and versatility of this field for the preparation and design of catalysts with interesting textural, structural, and chemical properties and for the understanding of catalytic performance. The preparative and physico-chemical properties of a pertinent selection of unitary titania xerogels are described and qualitatively compared with known titania high-temperature and low-temperature aerogels. The preparation, characterization, and catalytic performance of metal oxide–titania aerogels and metal–titania aerogels studied so far are summarized and shown to reveal prospective catalytic properties based on advantageous textural characteristics and novel redox as well as acid–base functionalities – accomplished by the control of composition and structure at molecular scale by means of sol-gel chemistry. In the future the beneficial use of aerogels as catalysts or supports will depend on the progress made in both tailoring the surface chemistry of these solids and overcoming some technical limitations on their application.

1. Introduction

1.1. Ceramic use of titania

Titania is a material of great interest, which mainly resides in its applications as pigment to give whiteness and/or opacity in paints, plastics, and paper [1]. The most important oxide of titanium is the dioxide which crystallizes in three structural polymorphs (rutile, anatase, brookite). Rutile is the thermodynamically preferred form at all temperatures. All three TiO_2 modifications exist as minerals and can be synthesized. In contrast to brookite, both anatase and rutile are produced commercially by virtue of their technological importance.

The predominance of TiO_2 as a pigment (rutile > 80%) is a consequence of its refractive index, lack of absorption of visible light, stability, nontoxicity, and ability to be manufactured in the desired size range. The ceramic applications of TiO_2 depend on its potential as an opacifier (use in enamels, matting agent), its

* Corresponding author.

[1] Present address: F. Hoffmann–La Roche Ltd., Vitamins and Fine Chemicals Division, Research and Technology Development, VFH, CH-4070 Basel, Switzerland.

0920-5861/97/$32.00
PII S0920-5861(96)00164-2

refractoriness in combination with its ease of sintering (thread guides), and the electrical properties of both TiO_2 and certain inorganic titanates (barium titanate with high dielectric constant, lead zirconate titanate with piezoelectric properties). As far as the structural ceramics are concerned, the wider use of TiO_2 has probably suffered from its low fracture toughness, which is about half that of alumina.

1.2. Catalytic use of titania

As a catalyst support for oxides, such as molybdena, tungsta, and especially vanadia [2,3], titania has many applications [2] – selective oxidation of hydrocarbons, decomposition of isopropanol, ammoxidation of aromatic hydrocarbons, selective catalytic reduction (SCR) of nitric oxide, and dehydration of N-ethylformamide with subsequent isomerization of the isonitrile to propionitrile.

In conjunction with group VIII metals titania exhibits the well known, reversible strong metal–support interactions, SMSI [4–6]. After elimination of the apparent (or indirect) metal–support effects, including inhibition of reduction of the metal by the support, specific particle size effects (size, epitaxial growth, morphology), bifunctionality, spillover, and effects of support action as a source or sink of catalytic poisons, real metal–support interactions, assigned to geometric and electronic effects, were identified by Tauster et al. [4,5] for "reducible" oxide-supported group VIII metals after reduction at high temperature (ca. 770 K). These geometric and electronic effects are likely to originate from the decoration of the metal by reduced, migrating MO_x-species, formation of intermetallic compounds, and/or electron transfers from the superficially "reduced" support to the d-band of the metal (i.e., localized charge transfers). Consequences, ascribed to these effects, are the drastic suppression in H_2- and CO-chemisorption capacity and changes in activity for structure-sensitive reactions (e.g., alkane hydrogenolysis), whereas only modest impacts on activity are observed for structure-insensitive reactions. Typically, the hydrogenation of aromatic and olefinic reactants decreases monotonically as the H_2 reduction temperature increases. As to the hydrogenation of carbonyl groups, however, in many cases the strong metal–support interactions are supposed to be the reason for favorable selectivity and/or activity [4–10], which become apparent even after reduction at low temperature.

Further research efforts are directed towards exploiting TiO_2-mediated photocatalysis [11]. Highly potent oxidants (holes) can be produced at semiconductor surfaces by illumination of wide-bandgap semiconducting materials, using light with higher energy than their bandgap. This photoexcitation of electrons is the cause of the photocatalytic activity. The degree of photoconduction depends significantly on the purity of the material employed. As to TiO_2, anatase and rutile are both electrical insulators at ambient temperature. However, since an empty conduction band, inferred from the empty Ti^{4+} $3d$-orbitals, lies only ca. 3 eV above the valence band, derived from the O^{2-} $2p$-orbitals, electrons may be promoted to the conduction band by radiation at wavelengths shorter than 410 and 385 nm for rutile and anatase, respectively.

1.3. Sol-gel–aerogel and catalysis

Prior to contemplating this section, it seems appropriate to present a list of salient literature, which provides a pertinent overview:

1. Sol-gel technology – Refs. [12,13].
2. Organometallic sol-gel precursors – Refs. [14–16].
3. Sol-gel in conjunction with the different variants of supercritical drying leading to aerogels – Ref. [17].
4. Physico-chemical properties (elasto-mechanical, optical, thermal, dynamic, and mass transport characteristics) as well as applications of aerogels, mainly based on silica – Ref. [18].

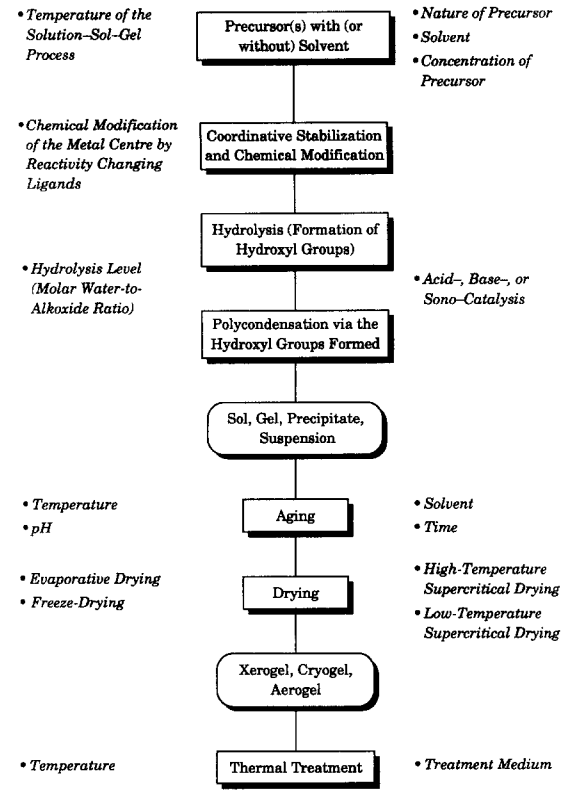

Fig. 1. Illustration of the sol-gel process with its highly controllable tools for tailoring the properties of solids.

5. Sol-gel method and catalytic materials – Refs. [17,19–21].
6. Aerogels in catalysis and physico-chemical properties relevant to catalytic applications – Refs. [17,19].

The motivation to combine the solution–sol-gel technique with the methods of supercritical drying for the preparation of aerogel catalysts and supports resides mainly in the highly controllable sol-gel technology together with the unique morphological and chemical properties induced by supercritical drying. Sol-gel chemistry, either by itself or in combination with supercritical drying, is a potent and versatile means for both the preparation and design of solids with novel structural and chemical properties and the understanding of catalytic performance. This versatility and potency is illustrated by the general scheme in Fig. 1.

The advantages of the sol-gel technology embrace the use of different wet-chemical tools for tailoring the synthesis and thus the resultant solid properties (i.e., large variety of synthetic parameters), high purity of the precursors, molecular-scale mixing of the components, homogeneity of sol-gel products with marked isotropy of chemical, physical, and morphological properties, ability to impose kinetic constraints and to stabilize metastable systems, and feasibility of a wide variety of solid shapes such as powders, spheres, fibers, monoliths, or membranes [17,21].

For supercritical drying two basic routes are nowadays applied – the high-temperature method and the various low-temperature techniques [17]. They both circumvent the destructive differential capillary stresses of conventional evaporative drying either by transferring the solvent into its supercritical state or by replacing the solvent mainly with supercritical CO_2, thus suppressing any liquid–vapor interface inside the sol-gel product. The critical constants of a few frequently used solvents are listed in Table 1. Although high-temperature supercritical drying via the direct transformation of the solvent into its supercritical state avoids capillary stresses, other destructive forces arise from the expansion of the liquid (permeability), contact with the autoclave liner wall, too high depressurization rates, and increased solvent reactivity. Especially the increased solvent reactivity at molecular scale, also termed "accelerated aging", accounts for severe structural

Table 1
Critical constants of selected solvents

Solvent	T_c (K)	P_c (MPa)
Freon® 116	293	3.0
CO_2	304	7.4
Diethylether	466	3.6
Acetone	508	4.6
Methanol	513	8.0
Ethanol	516	6.4
1-propanol	538	5.1
1-butanol	563	4.3
H_2O	647	22.0

Note. Data taken from Ref. [22].

and chemical changes. This accelerated aging often levels off the structural and chemical characteristics of the wet sol-gel products and thus favors the formation of "thermodynamically stabilized" aerogels. The main disadvantage of the high-temperature route is the stringent temperature impact (e.g., T_c for methanol 513 K; Table 1). The low-temperature methods overcome this restriction by extracting the sol-gel solvent by a fluid with much lower critical temperature such as CO_2 (T_c = 304 K; Table 1). Various studies on the influence of extraction conditions, including temperature, pressure, density, the use of either liquid or supercritical CO_2, and duration demonstrated that low-temperature supercritical drying is a dynamic process and the subtle gel network does not stay intact either (see Section 2.2.). Consequently, a variety of processes leads to significant changes in the wet-chemical structure of the sol-gel product, which, however, are generally "less drastic" compared to those induced by high-temperature supercritical drying.

In essence, although the sol-gel technology, both itself and in combination with supercritical drying, offers a potent means for the controlled preparation of solids with interesting textural, structural, and chemical properties, the technical application of sol-gel catalysts is hampered by the costs and, as to the aerogels in particular, by the manifold difficulties encountered in transferring them into an applicable form as well as the technical risks associated with supercritical drying. As regards the costs, risks, and technical constraints, promising alternatives are the use of inorganic salts or solid aggregates consisting of colloidal subunits, the subcritical preparation of aerogel-like materials, and the fixation of aerogels and aerogel-like materials on open-form supports or synthesis of composite materials [17]. The subcritical preparation of aerogel-like solids is spurred by a variety of methods reducing drying stresses, such as careful pore size control [17,23], aging [17], binders [17], organic templates [17,24], drying control chemical additives [17], exchange of the pore liquid by a liquid with lower surface tension, as well as surface modification with surfactants [17] or chemically bound compounds [25], and partial substitution of alkoxide precursors by adequate alkylalkoxy compounds [26].

2. Titania xerogels and aerogels

2.1. Sol-gel–xerogel

The advent of the sol-gel technique has opened different preparation routes for titania xerogels. A pertinent selection is quoted for comparison. Commercial TiO_2 P25 from Degussa is frequently employed as support material and thus provides the comparison basis. It possesses a BET surface area of ca. 50 $m^2\ g^{-1}$ and is prepared by flame hydrolysis of titanium(IV) tetrachloride.

Kozlowski et al. [27] hydrolyzed tetrabutoxytitanium(IV) in water at 343 K. After calcination at 673 K, the resulting titania possessed a BET surface area of 180 $m^2\ g^{-1}$ and contained anatase crystallites of 6 nm mean size. Unfortunately, the authors did not report on the pore size distribution.

For the preparation of titania sols as precursors for membranes, Lijzenga et al. [28] studied the influence of tetraisopropoxytitanium(IV) concentration (0.3–1 mol l^{-1} in isopropanol), amount of water (4.5–55 mol l^{-1} in isopropanol), and acid-to-alkoxide ratio for the peptization of the washed precipitate (0.35–0.6 with 1 M HNO_3). All these parameters were found to affect the size of the titania agglomerates in the peptized sols. This difference could be eliminated by ultrasonic treatment. The resultant titania membranes prepared with and without binder had BET surface areas of 109–156 and 13–31 $m^2\ g^{-1}$ after calcination at 573 and 773 K, respectively. The mean cylindrical pore diameter lay around 4 nm.

Barringer and Bowen [29] synthesized monodisperse titania powder by controlled hydrolysis of tetraethoxytitanium(IV) in ethanol. The mo-

lar ratio water-to-alkoxide (hydrolysis level, h) was always greater than 2.5 (0.1–0.2 M tetraethoxytitanium(IV), 0.3–0.7 M water). The ensuing washing with water by repeated centrifugation led to the formation of a surface coating with fine TiO_2 crystallites, resulting on the other hand in high specific surface areas of 250–320 $m^2\ g^{-1}$ after air drying. The pore diameters ranged from 1 to 6.5 nm. In contrast, washing with ethanol yielded only 8 $m^2\ g^{-1}$.

The process for the manufacture of porous ceramics described by Anderson and Xu [30] comprised hydrolyzing a titanium(IV) alkoxide in an aqueous solution with pH < 2 and manipulating the aqueous sol until a preselected pH was obtained, which readily resulted in different porosities after calcination at 773 K. Corresponding BET surface areas and porosities amounted up to 180 $m^2\ g^{-1}$ and 48%, respectively.

Moini [31] prepared titania xerogels by the hydrolysis of diisopropoxytitanium(IV) acetylacetonate in isopropanol–ethanol first at ambient conditions followed by hydrothermal treatment in an autoclave at 423 K. The initial hydrolysis level was ca. 28. Drying in air yielded amorphous titania with a BET surface area of 201 $m^2\ g^{-1}$. Unfortunately, the author did not report on the pore size distribution.

Montoya et al. [32] varied several wet-chemical solution–sol-gel conditions of the systems tetraisopropoxytitanium(IV) in isopropanol and tetraethoxytitanium(IV) in ethanol, principally working in the particulate regime [33] at hydrolysis levels of ≥ 8.9. The authors obtained BET surface areas of 93–647 $m^2\ g^{-1}$ after drying under vacuum at 353 K. Especially the xerogels with high surface area contained a significant amount of micropores. Calcination at 773 K caused crystallization and phase transformation as well as a drastic decrease in the BET surface areas to 9–113 $m^2\ g^{-1}$.

The uniform hydrolysis of different metal alkoxides via in situ homogeneous generation of water was investigated by Léaustic and Riman [34]. In the case of titania, hydrolysis was induced by sulfuric acid-catalyzed dehydration of t-butanol. After drying under vacuum at 323 K, the sulfate-containing titania xerogel possessed a BET surface area of 295 $m^2\ g^{-1}$. An extension of non-hydrolytic sol-gel processes was developed by Corriu et al. [35]. They added tetraisopropoxytitanium(IV) to either a solution of titanium(IV) tetrabromide or neat, liquid titanium(IV) tetrachloride and heated the solutions to 383 K in sealed vials. The as-prepared monolithic gels, derived from either titanium(IV) tetrabromide or titanium(IV) tetrachloride, were dried and calcined at 673 and 773 K, respectively. This thermal treatment resulted in anatase and BET surface areas of 158 and 180 $m^2\ g^{-1}$, respectively.

Roger and Hampden-Smith [36] prepared porous metal oxides via sol-gel type hydrolysis of metal alkoxides modified with one equivalent of polyacrylic acid ($h = 30$). After drying at 383 K, titania exhibited a BET surface area of 77 $m^2\ g^{-1}$ and an average pore diameter of ca. 4 nm. The removal of the polyacrylate template with nitric acid increased the BET surface area to 203 $m^2\ g^{-1}$ and mean pore diameter to ca. 10 nm. The specific micropore surface area was only 35 $m^2\ g^{-1}$.

2.2. Sol-gel–aerogel

The combination of sol-gel processing with supercritical drying offers the syntheses of titania aerogels with morphological and chemical properties that are not easily achieved by other preparation methods. A comprehensive survey of the literature about titania aerogels reflects the present state and demonstrates the principle differences compared to xerogels.

2.2.1. High-temperature aerogels

Teichner et al. [37,38] prepared titania aerogels by high-temperature supercritical drying. The authors studied the influence of the hydrolysis level, pH, concentration, and nature of alkoxide and concluded that alkoxide concentrations > 10 wt%, hydrolysis levels > 4, and

washing of the sol-gel product with fresh alcohol (removal of the reactive water) were necessary for the development of favorable textural properties. The resulting, uncalcined titania aerogel was X-ray amorphous and possessed a BET surface area of 168 $m^2\ g^{-1}$ as well as a specific pore volume of 0.45 $cm^3\ g^{-1}$. Unwashed, porous titania aerogel, containing anatase crystallites, was tested in the photocatalytic partial oxidation of isobutane [39]. Compared to non-porous forms of anatase, the aerogel yielded higher conversion of isobutane and lower selectivity to acetone.

Sanchez et al. [40] reviewed the influence of different relative rates of hydrolysis to condensation on the molecular structure as well as macroscopic appearance of titania sol-gel products (Table 2). Based on this survey, studies in our lab [41] about the effects of largely different relative rates of hydrolysis to condensation (Table 2) gave rise to distinctly different pore size distributions of the high-temperature aerogels calcined in air at 623 K. The graphically assessed pore size maxima ranged from 25 to 60 nm and the BET surface areas from 68 to 91 $m^2\ g^{-1}$. All titania aerogels, whether raw or calcined at 623 K, contained anatase crystallites of 13–19 nm mean size. In essence, the different relative rates did not reveal any obvious correlation with the textural properties. The larger mean crystallite sizes of the aerogels derived from either monodisperse or gelatinous precipitates were likely to reside in relatively fast condensation rate(s) and thus formation of dense colloidal primary-particles.

The sol-gel findings of Teichner et al. [37,38], which have been discussed above, and Yoldas [33] provided us the basis for another study on the preparation of high-temperature titania aerogels [42]. Yoldas [33] demonstrated that the evolution and precipitation of particulate material during the hydrolytic polycondensation of titanium alkoxides can be avoided by careful control of the molecular interactions, which is accomplished by the hydrolysis level, the molecular separation of the reactive species (dilution), and/or the presence of a critical amount of hydrochloric or nitric acid. The inorganic acids are relevant to the decoupling of hydrolysis and condensation (forced hydrolysis). Taking altogether [42], we showed that high-surface-area titania aerogels with prominent meso- to macroporosity can be synthesized via an acid-catalyzed sol-gel route with tetrabutoxytitanium(IV) and subsequent high-temperature supercritical drying. After calcination in air at 623 K, the titania aerogels possessed BET surface areas of nearly 200 $m^2\ g^{-1}$ and broad pore size distributions with maxima at ca. 50 nm. Changing the molar ratio of water/alkoxide/nitric acid from 4.1:1:0.08 to 4.2:1:0.12 had no marked effect on crystallinity, crystallite size, BET surface area, and porosity. Similarly, no impact was observed when the sequence of acid addition was changed (either acid to alkoxide solution or acid to hydrolysant prior to mixing).

An alternative approach to the conventional preparation of oxide powders was devised by Chhor et al. and Pommier et al. [43,44]. They exploited the specific properties of supercritical fluids as reaction medium, including high solubility, low viscosity, and high diffusivity, for the thermally induced decomposition of dis-

Table 2
Sol-gel products obtained according to the relative rates of hydrolysis to condensation

Hydrolysis	Condensation	Result	Sol-gel example
Slow	slow	colloid or sol	$Ti(t\text{-}OAm)_4$–t-AmOH
Fast	slow	polymeric gel	$Ti(OBu)_4$–AcOH, $Ti(i\text{-}OPr)_4$–HNO_3
Fast	fast	colloidal gel or gelatinous precipitate	$Ti(i\text{-}OPr)_4$–i-PrOH
Slow	fast	controlled precipitation	$Ti(OEt)_4$–EtOH

Note. Data quoted from Ref. [40].

solved precursors in a batch operation. The formation of solid particles was expected to occur with high nucleation rate and coagulation between particles, as to the prevailing growth mechanism. The recovery of the powder was finally achieved by isothermal depressurization, thus avoiding the liquid–solid separation steps of wet-chemical procedures. With regard to the synthesis of titania powder, the decomposition of tetraisopropoxytitanium(IV) in either ethanol or isopropanol (0.4 M) was accomplished after 2 h at 608 or 553 K, respectively. In the case of ethanol, the decomposition at 623 K for 2 h resulted in the formation of anatase, primary-particle sizes of 20–60 nm, "soft" agglomerates of 0.5–3 mm size, and BET surface areas of 40 $m^2\ g^{-1}$. Similar characteristics were observed for the preparation in supercritical isopropanol again at 623 K and 2 h reaction time. In addition, the concept of thermal decomposition of organometallic compounds in a supercritical fluid was applied to the dynamic or static deposition of titania films [45], derived from tetraisopropoxytitanium(IV) in isopropanol–CO_2 (molar ratio 0.5), on alumina substrates. The use of CO_2 as co-solvent lowered the critical temperature of the solvent and thus allowed the operation of the reactor at an initial temperature of 513 K. The final substrate temperature in the reaction vessel, adjusted with a separate heating cycle, was ca. 573 K. The high reactant solubility accounted for high concentration and hence high deposition rate. The as-received films were 1–5 mm thick, built up from particles of 200–400 nm size, and contained anatase as crystalline TiO_2 modification. However, under the experimental conditions studied, precise control of the film thickness below ca. 2–3 mm was not yet satisfactory.

Shin et al. [46] investigated the preparation of high-surface-area titanium oxynitrides via temperature-programmed nitridation of high-temperature titania and Rh–titania aerogels in flowing NH_3 at a final temperature of 958 K. The titania aerogels, prepared from either 30 or 50 wt% tetrabutoxytitanium(IV) in butanol and with modest BET surface areas of ca. 60 $m^2\ g^{-1}$, led to different degrees of nitridation, 76.9 and 52.9%, different BET surface areas, 62 and 46 $m^2\ g^{-1}$, and different phase compositions, TiN_xO_y and TiN_xO_y together with anatase, respectively. For the 2 wt% Rh–titania aerogel, prepared via hydrolysis of 50 wt% tetrabutoxytitanium(IV) in butanol with an appropriate aqueous solution of $RhCl_3$, the BET surface area decreased from 113 to 87 $m^2\ g^{-1}$ by virtue of nitridation, the degree of nitridation was 70.3%, and the phases present were TiN_xO_y as well as Rh.

Hunter et al. [47] stated that for the conversion of methane to methanol at $\geq$ 623 K and 30 atm the titania aerogel was too active and carried the oxidation reaction to CO and CO_2. No preparative and physico-chemical details of the titania aerogel used were reported.

Hrubesh and Pekala [48] examined the solid, gaseous, and radiative contributions to the thermal properties of organic and inorganic aerogels, including titania, in order to identify how to reduce the thermal conductivity of air-filled aerogels. The authors concluded that essential improvements in the insulative properties of aerogels may be achieved by the (i) use of materials with low intrinsic solid conductivity; (ii) reduction of average pore size; and (iii) increase in the infrared extinction (multi-component systems). (For the latter point, see Section 3.2.) As regards aerogel monoliths suitable for insulative applications, however, their utility suffers from the extreme fragility and low moduli. In order to overcome these stringent drawbacks, Ramamurthi and Ramamurthi [49] prepared aerogel matrix composites, consisting of a bulk or monolith aerogel matrix (TiO_2, ZrO_2, Al_2O_3, carbon, mainly SiO_2) reinforced with fibers, whiskers, wools, particles, foams, and honeycombs. The synthesis comprised the preparation of a mostly methanolic sol-gel solution, mixing of the reinforcing material with the sol-gel solution, aging to obtain a gel, complete submergence of the gel in chiefly methanol, and finally high-temperature supercritical drying.

The addition of reinforcing ingredients resulted in enhanced mechanical strength of the composite aerogel, allowing them to resist cracking, disintegration, and shrinkage during supercritical drying and to supersede moisture sensitivity, as well as interesting acoustic and thermal insulation characteristics. Moreover, the gel stabilization enabled high rates of heating, depressurization, and cooling for supercritical drying and thus accounted for faster processing times. For comparison, gel composites were also dried by exchanging the sol-gel solvent with liquid CO_2 and subsequent low-temperature supercritical drying. In contrast to the samples prepared via high-temperature supercritical drying, these low-temperature aerogel composites required curing at temperatures in the range 523–773 K (removal of organic residues and hydroxyl groups), were less robust, and needed essentially longer processing times.

2.2.2. Low-temperature aerogels

In the case of low-temperature supercritical drying, Ayen and Iacobucci [50] reported on the preparation of unitary, binary, and ternary oxide aerogels by means of low-temperature, semicontinuous extraction with supercritical CO_2. As-prepared titania aerogels possessed low crystallinity (anatase), BET surface areas in the range 600–750 $m^2\ g^{-1}$, and average cylindrical pore diameters of 15–18 nm.

Campbell et al. [51] systematically studied the effect of hydrolysis level, amount of nitric acid, and calcination temperature on the textural properties of titania low-temperature aerogels dried by semicontinuous extraction with supercritical CO_2 at 343 K and 20.7 MPa. The wet-chemical design was based on the acidic hydrolysis of tetrabutoxytitanium(IV) in methanol and was similar to the one described in Ref. [42]. In general, the uncalcined titania aerogels were X-ray amorphous up to 673 K and transformed from anatase into rutile in the range 873–1073 K. They had BET surface areas of up to 650 $m^2\ g^{-1}$ and specific pore volumes of up to ca. 2.1 $cm^3\ g^{-1}$. The pore size distribution ranged from 2 to 10 nm at temperatures ≤ 873 K. The effect of water and acid content on the BET surface area were examined after calcination in oxygen at 773 K. The variation of the water-to-alkoxide ratio (hydrolysis level, h) from 1 to 8 at an acid-to-alkoxide ratio of 0.1 resulted in a distinct maximum BET surface area at $h = 4$; on either side of this optimum hydrolysis level the BET surface areas dropped off precipitously. At $h = 4$, the acid-to-alkoxide ratio was varied from 0.05 to 0.175. Although the BET surface area was again significantly sensitive to the acid content, there was a wider range of acid-to-alkoxide ratios, 0.075–0.175, over which a high-surface-area aerogel could be made. In essence, an increase of the acid content yielded qualitatively the same effect on the BET surface area as a decline in the water content. Too high an acid content or too low a hydrolysis level produced soft gels, indicative of linear polymeric networks, whereas vice-versa the colloidal characteristics prevailed. With increasing calcination temperature up to 1073 K, both BET surface area and pore volume decreased drastically. In addition, the near parallel decline was in agreement with the basically invariable range of pore sizes. Calcination at 673 K induced a decrease in the BET surface area and specific pore volume to ca. 350 $m^2\ g^{-1}$ and ca. 0.9 $cm^3\ g^{-1}$, respectively.

The optimum conditions of the above studies [51], i.e., molar ratio of H_2O/tetrabutoxytitanium(IV)/HNO_3 = 4:1:0.125, were chosen by Brodsky and Ko [52] in order to show the effect of drying temperature on titania aerogels semicontinuously extracted with supercritical CO_2 and calcined at 773 K. The drying temperature, varied in the range 343–473 K, at a constant pressure of 20.7 MPa, seemed to exert a large effect on the pore volumes, pore size distributions, and crystallization behavior, whereas BET surface areas remained essentially constant at ca. 190 $m^2 g^{-1}$. A successive rise in the extraction temperature from 343 to 473 K increased the specific pore volume from ca. 0.6 to ca. 1.0 $cm^3 g^{-1}$ and broadened the pore size

distributions associated with a shift of their maxima to higher values. After heating in vacuum at 573 K, the titania aerogel extracted at 343 K remained X-ray amorphous, on the contrary the sample extracted at 473 K contained anatase crystallites. In conclusion, the higher drying temperature seemed to facilitate the crystallization of titania along with its particle growth.

For similarly prepared titania aerogels, i.e., molar ratio of H_2O/tetrabutoxytitanium(IV)/HNO_3 = 4:1:0.1, Dutoit et al. [53] demonstrated that the extraction temperature (273–369 K) at either constant CO_2 pressure or constant CO_2 density, use of either liquid or supercritical CO_2, extraction duration, and calcination temperature are crucial factors significantly influencing specific surface area, pore volume, and pore size distribution of the uncalcined titania aerogels. The effects of temperature are surveyed in Fig. 2. Extraction at temperatures in the range 283–323 K and at constant density of CO_2 (850 kg m^{-3}) as well as extraction duration of 16 h resulted in a maximum specific surface area and pore volume at an extraction temperature of 313 K (Fig. 2, top). At constant pressure of 30 MPa and extraction duration of 4 h, an increase of the extraction temperature from 273 to 369 K caused a monotonous rise in BET surface and a maximum pore volume at 323 K (Fig. 2, bottom). At first glance, these findings seemed to be in contrast to the results of Brodsky and Ko [52]. Note, however, that their studies were performed at CO_2 pressures of 20.7 MPa and covered a temperature range of 343–473 K. Moreover, the calcination at 773 K prior to analysis was likely to disguise the principal effects of the extraction temperature applied. A rise in extraction duration from 4 to 16 h at 30 MPa and 323 K led to an increase in BET surface area and decrease in both specific pore volume and average pore diameter. As concerns the use of either liquid or supercritical CO_2, the large effects on the appropriate BET surface areas, pore volumes, and pore size distributions, for samples uncalcined or calcined at different

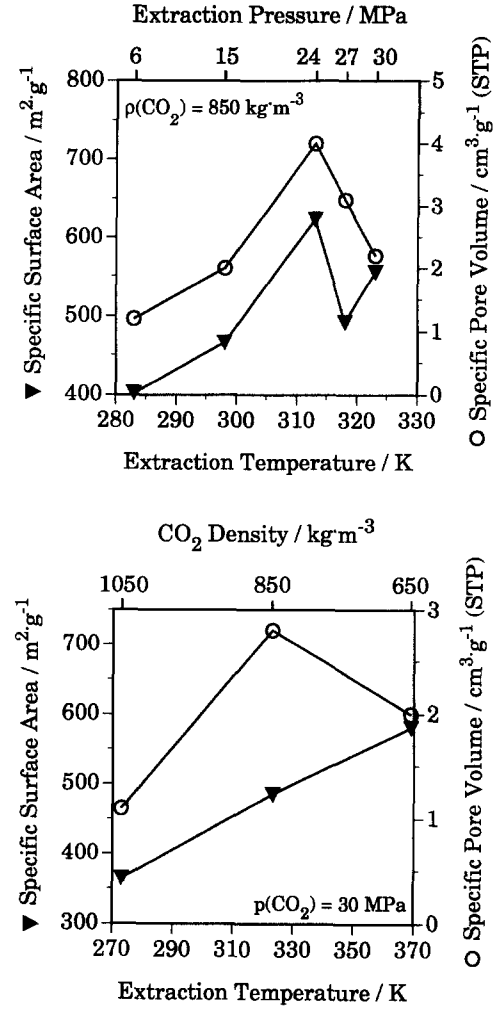

Fig. 2. Influence of the extraction temperature on specific surface area, ▼, and specific pore volume, O, of uncalcined aerogels at constant CO_2 density of 850 kg m^{-3} (top) and constant CO_2 pressure of 30 MPa (bottom). Data were determined by nitrogen physisorption at 77 K (STP; 273.15 K, 1 atm) and taken from Ref. [53].

temperatures, are represented in Fig. 3. When compared to the titania aerogels extracted with liquid CO_2, samples dried by supercritical CO_2 generally possessed higher BET surface areas and specific pore volumes, however, smaller maximum pore sizes. In the range of extraction conditions studied, all titania aerogels remained X-ray amorphous during calcination in air at $\leq$ 673 K. The remarkable carbon-contents in all uncalcined aerogels were not completely remov-

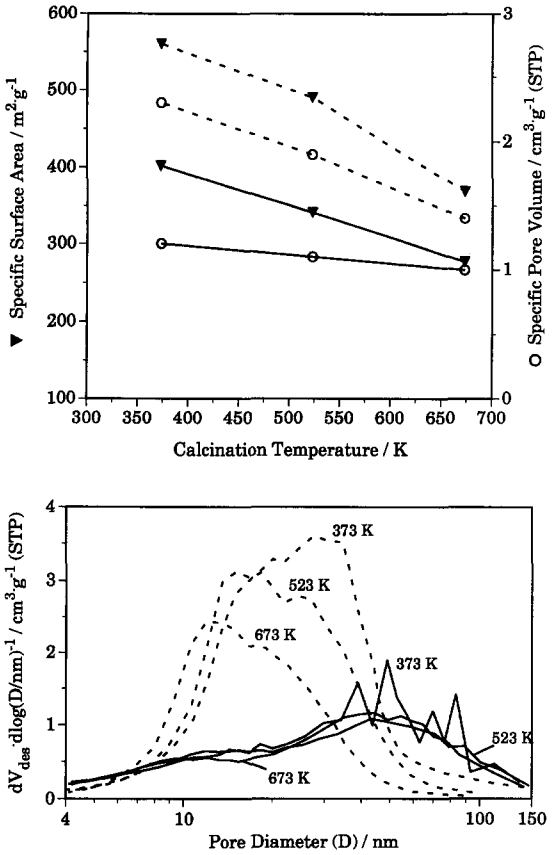

Fig. 3. Comparison of the textural properties of low-temperature titania aerogels semicontinuously extracted with either liquid (—) or supercritical (---) CO_2 and calcined in air at 373 (degassing temperature), 523, or 673 K. Top: specific surface areas (▼) and specific pore volumes (O); bottom: differential pore size distributions derived from the desorption branch of nitrogen physisorption. The extraction conditions applied were 6 MPa (CO_2 pressure) and 283 K (extraction temperature), —, or 30 MPa and 323 K, ---, respectively. Data were determined by nitrogen physisorption at 77 K (STP; 273.15 K, 1 atm) and taken from Ref. [53].

able by calcination at 673 K, carbon in quantities smaller than 1.5 wt% persisted in the samples. This residual carbon fully evolved only during calcination at 723 K, which was, however, associated with crystallization.

Dagan and Tomkiewicz [54] synthesized titania gels by mixing tetraisopropoxytitanium(IV) with anhydrous ethanol or isopropanol, water, and nitric acid. The molar ratio of alkoxide to nitric acid was kept constant (1:0.08), whereas the alcoholic solvent and the hydrolysis level were varied. After aging for at least twice the gelation time, the gels were washed with excess quantities of fresh alcohol. In some cases the alcohol washing was preceded by a water wash. For drying, the alcoholic solvent was replaced with liquid CO_2, which was finally released above its critical temperature. The non-annealed aerogels possessed BET surface areas of up to ca. 600 $m^2\ g^{-1}$ and were mesoporous. Annealing at 673–773 K caused a drop of the BET surface area to $\leq$ ca. 190 $m^2\ g^{-1}$. All non-annealed aerogels contained anatase crystallites of ca. 5 nm; after annealing the mean crystallite size amounted to ca. 7 nm. The application of these materials for the photodegradation of salicylic acid revealed higher photocatalytic activity for the non-annealed aerogels compared to those of corresponding annealed samples and commercial TiO_2 powder P25 from Degussa. This benign activity was suggested to reside in the high specific surface areas coupled with mesoporosity yielding enhanced adsorption capacity. According to the above procedure [54], Zhu and Tomkiewicz [55] prepared an acid-catalyzed titania aerogel (h = 4, tetraisopropoxytitanium(IV)/HNO_3 = 0.08) and characterized the morphology and microstructure using a variety of complementary techniques, including electron microscopy, nitrogen physisorption, small angle neutron scattering, and X-ray diffraction. The as-derived morphology consisted of spherical titania primary-particles of ca. 5 nm, which are closely packed into loosely aggregated secondary-mesoaggregates of ca. 50 nm.

2.3. Summarizing qualitative comparisons between xerogels and aerogels

The following comparisons reside in evaporatively (''conventionally'') dried xerogels and do not include subcritically prepared aerogel-like materials. (For details, see Section 1.3.)

A principal difference between xerogels and aerogels originates from the morphology [17]. A structure of branched and interconnected pri-

mary-particles, which form ultrafine cells (< 100 nm), is characteristic for aerogel materials and often described by the concept of self-similarity (fractal geometry [56]). In the case of xerogels, prepared by conventional drying (temperature and/or vacuum), various detrimental forces are active, causing differential microscopic and macroscopic shrinkage. The drying stress creates significant changes in surface area, pore volume, pore size, pore morphology, or bulk density. Thus xerogels usually show the effects of collapse and aggregation–densification during evaporation, which leads to denser morphologies with sharp edges and terraces. Macropores are usually present in aerogels and absent in xerogels. The morphologies of the ultrapores are significantly different. The ultrapores in aerogels are more open, whereas in xerogels they are closed. This behavior is further reflected by the marked shrinkage of xerogels compared to the corresponding aerogels in the course of drying. The distinct differences in the morphologies are also evident from the textural properties [17]. The isotherms observed with xerogels often fall into the type-I category (Langmuir type), which is generally found with microporous solids; whereas the isotherms observed with aerogels frequently fall into the type-IV category, which is very common among mesoporous solids. Thus, aerogels are usually meso- to macroporous with little microporosity and possess higher specific surface areas compared to the corresponding xerogels with prevailing micro- to mesoporosity. For the aerogels these catalytically favorable textural properties result in high accessibility of the dominating contribution of "internal" surface area and consequently availability of the active sites.

Crystallinity is often much higher for high-temperature aerogels compared to xerogels and low-temperature aerogels [17]. With binary or higher systems, the elevated temperature (> ca. 510 K), associated with enhanced solvent reactivity of high-temperature supercritical drying, helps to induce segregation–crystallization, which results in minor dispersion and thus significant structural and chemical differences compared to xerogels and low-temperature aerogels. (For further details, see Section 3.2.)

Purity is usually claimed to be one of the advantages of the sol-gel technology. This view has to be restricted to the precursors used, usually metal alkoxides [17]. After drying, the content of organic residues, due to the organic components involved in the sol-gel process (i.e., solvent, ligands, and modifiers), is usually smaller with high-temperature aerogels compared to low-temperature aerogels and xerogels [17]. These organic contaminants are attributed to realkoxylation of the surface, incorporation of ligands, and (physisorbed) solvent. The first contribution prevails with high-temperature aerogels, responsible for the hydrophobicity of such materials, and the latter in the case of low-temperature aerogels or xerogels. In the presence of reducible components, organic oxidation products and organic species, decomposed over metal formed, must also be taken into account. In essence, the amount, nature, and location of these remnant organic residues depend strongly on the drying method applied. As to their removal [17], studies on different aerogels showed that careful heat treatments up to ca. 600–800 K are required to remove the majority of these organic residues; however, a non-negligible part can still persist in the aerogels. This residual part can significantly influence the physical and chemical properties of an aerogel, such as the crystallization behavior or the catalytic activity by partially covering the active sites. In order to remove most of the organic residues prior to calcination, thus avoiding uncontrolled burn off and concomitant sintering, aerogel samples should first be treated in an inert gas flow or vacuum oven.

2.4. Summarizing qualitative comparisons between high-temperature and low-temperature supercritically dried aerogels

When compared to low-temperature supercritical drying, high-temperature supercritical

drying leads to thermodynamically more stable aerogel materials, which is reflected by prominent structural and chemical changes (see Section 1.3.). In general, the specific surface areas are higher with low-temperature aerogels than with high-temperature aerogels. However, with increasing calcination temperature this behavior vanishes and may even be inverted.

As mentioned above, high-temperature aerogels show marked propensity to segregation and/or crystallization. Corroborative evidence arises from the comparison between high-temperature and low-temperature titania aerogels. Anatase is observed in the case of as-received high-temperature aerogels, whereas the low-temperature aerogels remain X-ray amorphous up to 673 K.

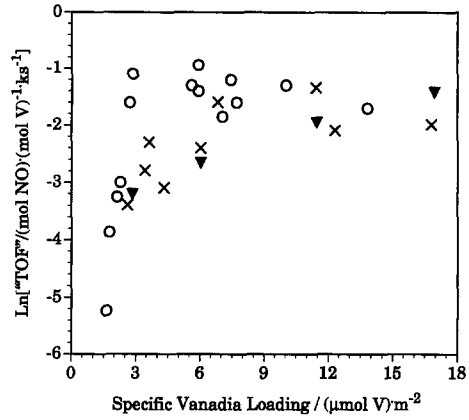

Fig. 4. Dependence of the specific activity of different titania-based vanadia catalysts for the selective catalytic reduction of NO with NH_3 on the specific vanadia loading. ×, vanadia grafted on various titania high-temperature aerogels, data from Ref. [57]; ○, vanadia grafted on P25 (Degussa) and titania xerogel prepared via an acid-catalyzed sol-gel route, data from Ref. [58]; ▼, vanadia–titania high-temperature aerogels directly synthesized via a two-stage sol-gel process, data from Ref. [59]. Reaction rates referred to the overall vanadium content ("TOF") were determined under differential conditions at 423 K.

3. Metal oxide–titania aerogels

3.1. Vanadia–titania and vanadia–niobia–titania aerogels

As to the immobilization of vanadium(V) oxide triisopropoxide [57], either chemical vapor deposition or grafting from non-aqueous solutions on different titania high-temperature aerogels [41] were applied in our lab [57]. The high specific surface areas of up to 200 $m^2\ g^{-1}$ accounted for the immobilization of larger amounts of active vanadia species per gram support, i.e., up to 17 wt% nominal V_2O_5. This benign behavior led to higher overall activities for the selective catalytic reduction of NO by NH_3 compared to catalysts based on medium-surface-area titania (P25 from Degussa with up to ca. 3 wt% V_2O_5). The dependence of the specific activity on the surface concentration of vanadia is shown in Fig. 4 together with literature data from Ref. [58] for P25- and titania xerogel-supported vanadia catalysts and from Ref. [59] for directly synthesized vanadia–titania aerogels. In the case of the vanadia on titania–aerogel catalysts, maximum specific activity was obtained at a surface concentration of ca. 7 (μmol V) m^{-2}. Higher loadings resulted in slightly lower specific activity and formation of three-dimensional V_2O_5, whereas lower coverages led to a remarkable loss in activity. The latter aspect paralleled with the marked structure sensitivity of the activity, corroborated by complementary vibrational and catalytic studies, and is in agreement with the results from Ref. [58]. The intrinsic activity depended mainly on the vanadia (surface) concentration, whereas the morphology and acidity of largely different titania supports seemed to exert only little influence.

Compared to the classic preparation of supported oxide(s) of first forming the support followed by the immobilization of the precursor(s) [57], sol-gel chemistry offers the introduction of the desired components during the wet-chemical stage, resulting in a one-step procedure. Our direct preparation of binary vanadia–titania aerogels with surface areas of ca. 200 $m^2\ g^{-1}$ and nominal loadings of V_2O_5 up to 30 wt%, via a two-stage sol-gel process with ensuing high-temperature supercritical drying, re-

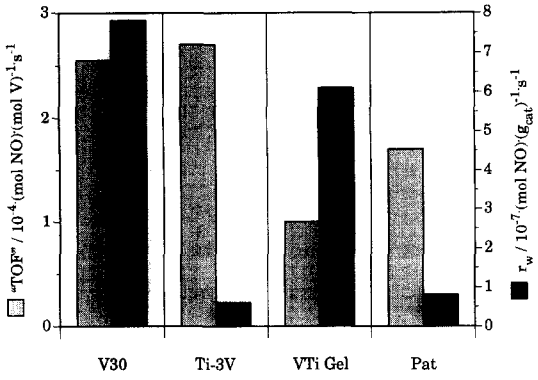

Fig. 5. Comparison of reaction rates per overall vanadium content ("TOF") and reaction rates per gram of catalyst (r_w) at 423 K of a high-temperature vanadia–titania aerogel *V*30 (30 wt% V_2O_5) with pertinent literature data. Ti–3V, vanadia grafted on titania P25 (Degussa) with 1.8 wt% V_2O_5; VTi Gel, binary xerogel prepared via a two-stage sol-gel process with 53 wt% V_2O_5; Pat, sequential precipitation according to the Mitsubishi Patent with 4.8 wt% V_2O_5. Data were taken from Ref. [59].

sulted in high dispersion and accessibility of the active vanadia component [59,60]. The beneficial use of high surface area in conjunction with high loading and accessibility is illustrated in Fig. 5. The reaction rate per overall vanadium content ("TOF") was similar to that of highly dispersed multiply grafted vanadia on titania catalysts. This result indicated that the vanadia phase, uniformly distributed in the three-dimensional gel network, was well dispersed and exhibited an activity similar to the multiply grafted vanadia species. The clear advantage of the aerogel catalysts resided in the higher loading that could be achieved, and consequently in higher reaction rates per catalyst weight. In addition, the variation of several sol-gel and drying parameters did not affect the resultant properties essentially, exemplifying the levelling of inherent wet-chemical differences over a wide range by high-temperature supercritical drying. Note that prior to catalytic testing in a fixed-bed microreactor the aerogel powders were agglomerated at 2–3 MPa, which proved to be sufficient to yield fairly stable granules leaving the textural properties virtually unchanged. This behavior was based on strong interparticular forces. The achievement of the desired exposition of highly dispersed active vanadia resided in the "preformation" of the titania matrix, enhanced segregation of the two constituents, spreading of the vanadia phase [3], and, when vanadia nuclei were formed, preferential heterocoagulation of vanadia nuclei and particles at slightly acidic conditions. As to the "preformation" of the titania matrix, studies on the redispersion of titania gel, prepared according to the procedure of aerogel C in Ref. [42] (H_2O/tetrabutoxytitanium(IV)/HNO_3 = 4.1:1:0.08, in methanol), with additional fresh methanol and subsequent high-temperature supercritical drying of the resultant sol showed that the textural and crystallographic properties of the as-received dry titania aerogel were virtually not affected. Consequently, this essential finding rendered the homogeneous introduction of another component to the preformed "colloidally" distributed titania feasible and could be transferred to the preparation of multi-component systems. As concerns the enhanced segregation, the higher sol-gel reactivity of tetrabutoxytitanium(IV) compared to vanadium(V) oxide tri-iso- or tri-n-propoxide together with the effects of high-temperature supercritical drying clearly accounted for the segregation and, in the case of high-temperature supercritical drying, spreading of vanadia on the surface of titania cores. With regard to the ratio of homocoagulation to heterocoagulation of the vanadia nuclei, the acidic pH of the sol-gel solution was likely to lead to positively charged titania particles and negatively charged vanadia clusters owing to the distinctly different points of zero charge [$pH_{pzc}(TiO_2) \approx 4.5–6.3$, $pH_{pzc}(V_2O_5) \approx 1.4$].

DRIFT studies about the vanadia–titania high-temperature aerogels [61] and vanadia on titania-aerogel catalysts [57] revealed that for the selective catalytic reduction of NO with NH_3 Brønsted-bound ammonia was involved. In addition, the specific activities correlated with the fraction of Brønsted-bound ammonia on the active vanadia constituent. This fraction significantly increased with the vanadia loading of the aerogels. Such a behavior reflected the structure sensitivity of both the NH_3 adsorption and the

activity (Fig. 4). Note that on unitary titania aerogel mainly Lewis-bound ammonia was observed. In conclusion, these results together with the interesting acidic properties of niobia prompted us to prepare ternary niobia-containing vanadia–titania high-temperature aerogels [62], closely following the preparative concept of the binary vanadia–titania aerogels with 20 wt% V_2O_5 [59]. Although the loading of nominal Nb_2O_5 was increased from 0 to 6 wt%, the textural, structural, and catalytic properties of the aerogel samples calcined at 573 K were almost not influenced. This invariability indicated physical separation of the vanadia and niobia components, forming isolated islands of clusters with only negligible adlineation. An increase of the calcination temperature to 723 K led to temperature-induced migration–agglomeration of the vanadia component, giving rise to two-dimensionally connected patches and even three-dimensional multi-layered structures. This behavior was similar to the binary vanadia–titania aerogel catalysts calcined at ≤ 673 K. The calcination at 723 K, however, resulted in crystallization of the vanadia phase and concomitant anatase-to-rutile transformation. The presence of niobia was likely to retard both the crystallization of vanadia and phase transformation of anatase, hence favoring further migration–agglomeration with the simultaneous build-up of more active vanadia nuclei, as suggested by the results in Fig. 6.

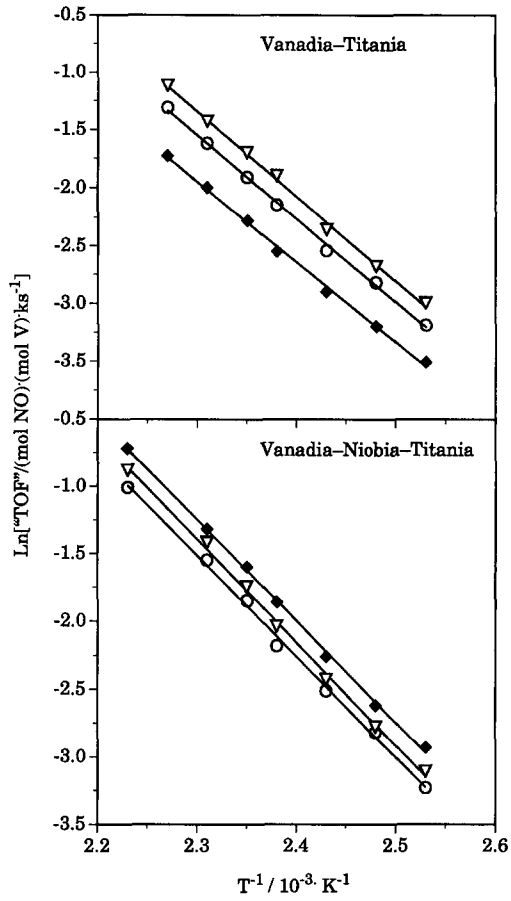

Fig. 6. Effect of vanadia stabilization by niobia in vanadia–titania high-temperature aerogel catalysts, calcined at different temperatures, on the Arrhenius plots of the specific reaction rates, determined under differential conditions. Top: vanadia–titania aerogel catalysts with 20 wt% nominal V_2O_5 [59]; bottom: vanadia–niobia–titania aerogel catalysts with 20 wt% nominal V_2O_5 and 6 wt% nominal Nb_2O_5 [62]. ○, calcined in air at 573 K; ▽, calcined in air at 673 K; ◆, calcined in air at 723 K.

3.2. Silica–titania aerogels

Ti-silicalites (TS-1), which represent potent and versatile redox zeolites, suffer from the steric restriction in the microporous structure (small channel size of ca. 0.55 nm). This limitation prevents their application in the field of fine chemistry and thus spurred us to devise prospective large-pore catalysts [63,64]. As to the synthesis, an acidic hydrolysant was added to a solution of tetramethoxysilicon(IV) and tetraisopropoxytitanium(IV) precedingly modified by acetylacetonate in isopropanol. The sol-gel conditions varied were the hydrolysis route chosen, i.e., prehydrolysis in addition to chemical modification and acid catalysis, as well as the amount of nominal TiO_2 (≤ 20 wt%). The resultant silica–titania gels were dried by different methods, including conventional drying (373 K), high-temperature supercritical drying (533 K), and extraction with supercritical CO_2 (313 K). The benign Ti-dispersion at molecular scale, i.e., both structure and composition, together with meso- to macroporosity was achieved by carefully matching the alkoxide reactivities via chemical modification along with acid-catalysis

and subsequent semicontinuous extraction of the solvent with supercritical CO_2 at 313 K and 24 MPa. The benefit of both large pores and high Ti-dispersion for the epoxidation of cyclohexene with cumene hydroperoxide is illustrated by the differently dried silica–titania materials in Fig. 7. The low-temperature and high-temperature aerogels possessed meso- to macroporous pore size distributions with maxima at ca. 55 and 60 nm and specific pore volumes of 1.7 and 3.6 $cm^3\ g^{-1}$, respectively. The porosity was most likely to resist the capillary forces during rewetting. In contrast, the xerogel was microporous with a pore size maximum < 2 nm and a mesopore volume of ca. 0.03 $cm^3\ g^{-1}$, indicative of the destructive capillary forces occurring during conventional evaporative drying. With regard to the Ti-dispersion derived from vibrational analysis of the generic Si–O–Ti band at ca. 940 cm^{-1}, the low-temperature aerogel and xerogel possessed significantly better Ti-dispersion compared to the high-temperature aerogel. Altogether, only the low-temperature aerogel combined marked accessibility with highly dispersed Ti. This favorable combination resulted in the highest activity and selectivity for epoxide formation among the differently dried silica–titania catalysts [63,64]. The activity of the low-temperature aerogel significantly surpassed the one of Ti-substituted silicalite TS-1, which distinguishes itself by optimum Ti-dispersion and very narrow channels of ca. 0.55 nm [64]. Note that not cyclohexene but cumene hydroperoxide is the bulkiest molecule ($0.55 \times 0.63 \times 0.93$ nm). Moreover, the selectivity of the high-temperature aerogel was almost as good as that of the low-temperature aerogel. In contrast, the xerogel induced some peroxide decomposition with negligible selectivity to epoxide formation. Prehydrolysis of the less reactive tetramethoxysilicon(IV) in conjunction with chemical modification and acid catalysis generally led to lower porosity, but did not affect the Si–O–Ti heteroconnectivity. In the case of the low-temperature aerogels, a rise in nominal TiO_2 content from 2 to 20 wt% resulted in lower microporosity, higher BET surface area ($\leq$ ca. 700 $m^2\ g^{-1}$), and an essential increase in the overall contribution of Si–O–Ti species, altogether culminating in a maximum initial rate per gram of catalyst for the low-temperature aerogel with 20 wt% nominal TiO_2. Note that all materials studied gave rise to excellent structural and textural stability up to 873 K in air.

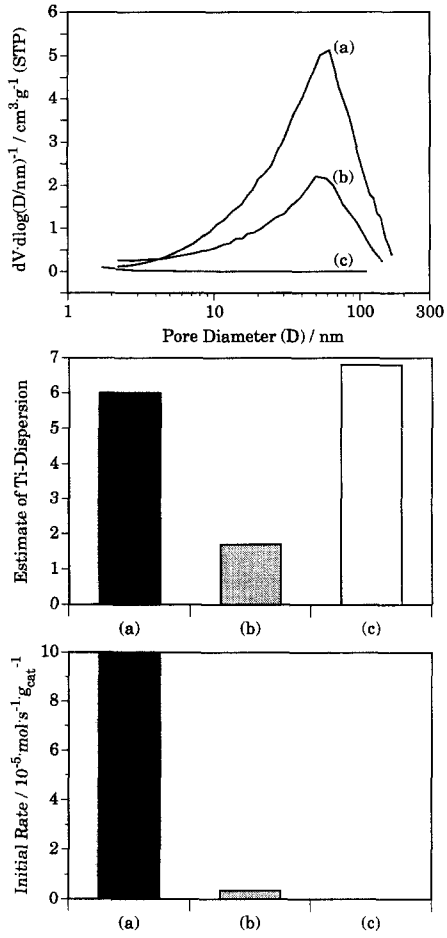

Fig. 7. Differently dried titania–silica mixed oxides with 10 wt% nominal TiO_2 and calcined in air at 673 K. Top: differential pore size distributions derived from nitrogen physisorption at 77 K (STP; 273.15 K, 1 atm) [63]; middle: estimates of Ti-dispersion derived from vibrational spectroscopy and Eq. (1) in Ref. [63]; bottom: initial rates for the epoxidation of cyclohexene with cumene hydroperoxide at 333 K [64]. (a) low-temperature aerogel, (b) high-temperature aerogel, and (c) xerogel.

As regards the influence of the drying method on Si–O–Ti heteroconnectivity, similar results were obtained by various studies [65–71], which

were mainly prompted by the interesting physico-chemical characteristics of silica–titania mixed oxides, including acoustic impedance matching, transparency, thermal insulation (titania constituent as infrared opacifier), and low coefficients of thermal expansion. Cogliati et al. [66] obtained silica–titania xerogels and aerogels containing ≤ 30 mol% titanium (36.3 wt% TiO_2), from tetramethoxysilicon(IV) and either titanium(IV) tetrachloride or tetraisopropoxytitanium(IV). The aerogels were supercritically dried at high temperature in alcohol ($T = 543$ K) and dried at low temperature in CO_2 ($T = 313$ K). Again, high-temperature supercritically dried samples exhibited anatase segregation at all concentrations and temperatures. Aerogels obtained from low-temperature supercritical drying, however, remained completely homogeneous up to 7 mol% (9.1 wt% TiO_2) of titanium and temperatures ≤ 1473 K. Xerogels showed the same behavior up to only 3 mol% of TiO_2 (4 wt% TiO_2). Note that the studies in Ref. [63], and especially Refs. [70,71] resulted in higher Ti-dispersion for the corresponding xerogels. Calvino et al. and Bernal et al. [70,71] prepared silica–titania gels with up to 10 mol% TiO_2 either by mixing an ethanolic solution of tetraethoxysilicon(IV), H_2O, and HCl ($h = 4$) with butanolic tetrabutoxytitanium(IV) modified by acetic acid (acetic acid/tetrabutoxytitanium(IV) = 5.5) or via prehydrolysis of the tetraethoxysilicon(IV)-containing solution under ultrasound and subsequent addition of the modified titania precursor. The as-received gels were dried by evaporative drying (300 K), exchange in two steps with isoamyl acetate and further low-temperature supercritical drying with CO_2 (315 K, 7.5 MPa), or high-temperature supercritical drying (600 K). After calcination at 773 K, all three samples exerted interesting activity for the gas-phase dehydration of *t*-butanol to isobutene at 373 K based on Lewis-type acid sites. The strong effect of the drying method was again reflected by the decline in Si–O–Ti heteroconnectivity, derived from XRD, FTIR, and XANES, in the order: xerogel > low-temperature aerogel > high-temperature aerogel. The same trend was followed by the surface acidity. In the case of high-temperature supercritical drying, the authors concluded that the elevated drying temperature of 600 K was likely to induce Ti-leaching with ensuing redeposition in the narrower pores, essentially modifying both the textural and surface chemical properties of the resultant material. Moreover, an increase in loading from 0 to 10 mol% TiO_2 paralleled with a rise in activity for dehydration. In contrast to the results of Ref. [63], the low-temperature aerogels with 10 mol% TiO_2 and calcined at 773 K contained anatase crystallites. Note that Dutoit et al. [63] reported that the aerogels with 20 wt% TiO_2 remained X-ray amorphous up to 873 K. This difference highlights that the modification by acetic acid is not as efficient as the modification by acetylacetonate, which forms a bidentate chelate complex. Prehydrolysis under ultrasound generally led to lower Ti-dispersion and activity compared to the corresponding samples without ultrasonically assisted prehydrolysis. In the case of high-temperature aerogels, the effect of prehydrolysis under ultrasound on textural properties and ultrastructural evolution during sintering was examined in more detail in Refs. [72,73]. As to the textural properties, higher BET surface areas, lower pore volumes, finer and sharper pore size distributions, and lower average particle sizes were achieved by means of prehydrolysis under ultrasonic treatment.

The potential of prehydrolysis together with acid-catalysis of the less reactive silica precursor was applied by Miller et al. [74] for the preparation of silica–titania low-temperature aerogels semicontinuously extracted at 343 K and 22 MPa. Either tetrabutoxytitanium(IV) was added to prehydrolyzed tetraethoxysilicon(IV) in methanol along with nitric acid or both precursors were introduced simultaneously to the acidic, methanolic hydrolysant (non-prehydrolysis). In essence, prehydrolysis led to higher activity for the isomerization of 1-butene in gas phase at 423 K, higher acid site density, and

higher fractional Brønsted-site population for the mixed oxides calcined at 773 K than those of the corresponding non-prehydrolyzed samples. All of the mixed oxides possessed predominantly Lewis acid sites. In the titania-rich end of the composition range, the fractional Brønsted-site population increased linearly with the silica content for both the prehydrolyzed and non-prehydrolyzed aerogel series. In the middle of the composition range, however, the slopes of both curves decreased markedly. Furthermore, the higher the silica content, the more effective was the retardation of both crystallization into anatase and anatase-to-rutile transformation, for both aerogel series. Iacobucci et al. [50,75,76] reported on the synthesis of silica-rich and titania-rich low-temperature aerogels–taking ca. 13 and 96.5 wt% nominal TiO_2 mixed oxides as examples. The latter [75] was manufactured by prehydrolysis of tetraethoxysilicon(IV) in isopropanol–water associated with HCl and HF ($h = 6$). After adjusting the pH to 4.5 with HCl, tetraisopropoxytitanium(IV) was added. The resultant fibrous gel was semicontinuously extracted with supercritical CO_2 at 313 K and 24.6 MPa. After additionally drying at 353–373 K, the final product had a BET surface area of 668 $m^2\ g^{-1}$. In contrast, the silica-rich aerogel [76] was prepared by the addition of the acidic hydrolysant to an isopropanolic solution of tetraethoxysilicon(IV) and tetraisopropoxytitanium(IV), aging of the white solution at 353 K, and, after gelation, at room temperature, as well as ensuing semicontinuous extraction with supercritical CO_2 at 313 K and 17.5 MPa. After drying at 353–373 K, the BET surface area amounted to 872 $m^2\ g^{-1}$. Cogliati [65] prepared spherical silica–titania aerogel microbeads of 150–200 mm with 2 wt% nominal TiO_2. Tetraethoxysilicon(IV) was introduced to a solution composed of ethanol, water, and HCl at 323 K. After this prehydrolysis step, the titania precursor, either tetraisopropoxytitanium(IV) or titanium(IV) tetrachloride, was added. The hydrolysis level was ca. 1. After cooling the solution to 285 K, hydrolysis was completed by additional water diluted in ethanol, giving rise to an overall hydrolysis level of 5. The as-received colloidal solution was evaporated to ca. half the volume and subsequently transferred into a decanolic microemulsion. After gelation of the sol droplets, the gel particles were washed with acetone, statically extracted by liquid CO_2, and finally low-temperature supercritically dried at 313 K. The silica–titania aerogel particles were X-ray amorphous and possessed BET surface areas of ca. 920 $m^2\ g^{-1}$. The pore diameters ranged from 5 to 8 nm. Pazol and DeFranzo [77] prepared monolithic silica–titania high-temperature aerogels with 12.5 wt% nominal TiO_2 for lightweighted ultra-low-expansion optics. After the prehydrolysis of tetraethoxysilicon(IV) in ethanol–water under reflux at 323 K, tetraisopropoxytitanium(IV) was added and, after a second reflux period, gelation was forced by the introduction of base. Subsequently, the gel monoliths were supercritically dried at 573 K applying nitrogen prepressure.

3.3. *Zirconia–, niobia–, alumina–, magnesia–, silica–yttria–, and alumina–yttria–titania aerogels*

A comprehensive survey of additional examples for titania-based oxide aerogels highlights the potential of sol-gel mixed oxides as to the generation of prospective structural, chemical, and catalytic properties.

Weissman et al. [78] investigated zirconia–titania aerogels as support precursor for hydrotreating catalysts based on sulfided molybdenum and nickel. A solution of tetrabutoxytitanium(IV), tetrapropoxyzirconium(IV), and small amounts of HNO_3 in propanol was mixed with water diluted in propanol. In dependence on the composition, the overall hydrolysis level and content of acid were 2.1 and 0.026 for the sample with 85 wt% nominal TiO_2, and 1.97 and 0.042 for the one with 26 wt% TiO_2, respectively. The as-received gels were semicontinuously extracted with supercritical CO_2 at

343 K and 20.7 MPa. After subsequent calcination at 773 K, the low-temperature aerogels were mixed with water into a paste, extruded and calcined at 673 K to form hardened extruded catalyst supports. This extrusion process resulted in a marked decrease in BET surface area from 390 to 120 $m^2\ g^{-1}$ and 315 to 205 $m^2\ g^{-1}$ for the samples with 85 and 26 wt% TiO_2, respectively, as well as in crystallization. The crystallization was, however, not as extensive as in the single component materials, which reflected an intimate mixing of the binary systems limiting adverse changes due to heating. Corroboration for this favorable interaction arose from the significantly enhanced surface acidity of the zirconia–titania aerogels after calcination at 773 K, with the maximum occurring at 50 wt% TiO_2. As concerns the manufacture of the catalyst for hydroprocessing gas oil, molybdenum and nickel in aqueous solutions were deposited onto the supports by incipient wetness, followed by drying at 383 K and calcining at 673 K. The loadings corresponded to 2 wt% Ni and 6 wt% Mo. Although the reaction temperature for hydrotreating was 200 K lower than the highest calcination temperature used in the preparation of the catalysts, the supports derived from low-temperature aerogels were not stable under reaction conditions, suffering from a significant loss in BET surface area and showing an increase in crystallinity after exposure to hydrotreating conditions. The catalysts with a prevailing content of zirconia were exceptionally prone to collapse, forming low-surface-area material having almost no catalytic activity. Materials with higher titania content, however, exhibited higher activities for hydrodesulfurization and hydrodenitrogenation related to the surface area and higher activity and selectivity in hydrodenitrogenation relative to the volume than a conventionally prepared catalyst supported on alumina.

In the case of niobia–titania [79], aerogel synthesis is an effective way to both prepare acidic, high-surface-area niobia-containing materials and, for maximizing the acid strength, prevent niobia, either by itself or in combination with another oxide, from crystallization induced by thermal treatment. Upon vigorous stirring a well-mixed solution of methanol, doubly deionised water, and nitric acid was added to niobium(V) pentaethoxide and titanium(IV) tetrabutoxide dissolved in methanol in the desired ratio. The resultant clear, firm gel was subsequently extracted with supercritical CO_2 at 343 K and 20 MPa. After calcination in oxygen at 773 K, the niobia–titania aerogels with 29.4, 62.5, 86.9, or 100 wt% nominal Nb_2O_5 possessed BET surface areas of 190–280 $m^2\ g^{-1}$. All samples were X-ray amorphous with the exception of the titania-rich material, which contained poorly crystalline anatase. Titration with n-butyl amine and isomerization of 1-butene provided evidence for both Lewis and Brønsted acid sites. Moreover, the acid site distributions were not a strong function of composition. Calcination of unitary niobia at 873 K resulted in the crystallization of TT-Nb_2O_5 and concomitant elimination of the highest acid strength ($pK_a = -8.2$). The BET surface area decreased from 190 to 60 $m^2\ g^{-1}$. Further heating to 1073 K formed T-Nb_2O_5 and eliminated all acid sites below a pK_a-value of $+1.5$; in addition, the BET surface area dropped further to 5 $m^2\ g^{-1}$. As to the mixed oxides, however, only calcination at 1073 K led to segregation–crystallization of Nb_2TiO_7 coupled with a decline in BET surface area to 25–40 $m^2\ g^{-1}$ and loss of strong acid sites. Besides the rigid, porous network of an aerogel slowing down the kinetics of sintering and crystallization, the interaction of niobia with another oxide additionally favors the stabilization of amorphous niobia. A co-precipitated xerogel with 62.5 wt% Nb_2O_5, prepared for comparison by adding NH_4OH dropwise to a methanolic solution of the alkoxides, had a BET surface of 15 $m^2\ g^{-1}$ and contained anatase after calcination at 773 K. Despite these prominent differences compared to the corresponding aerogel, the xerogel gave rise to very similar acid site distributions. This similarity suggests that the acidity is

related to niobia being stabilized from crystallization by the interaction with another oxide accomplished by either co-precipitation or aerogel synthesis; the latter approach had the added benefit of providing a high-surface-area material. Compared to silica immiscible with niobia, titania is less effective as a structural stabilizer at higher temperatures (≤ 1073 K), because it tends to form Nb_2TiO_7.

Teichner et al. [38] prepared magnesia–titania aerogels from a solution of titanium(IV) tetrabutoxide (5 wt%) and magnesium(II) dimethoxide (1.25 wt%) in benzene/methanol (11.5:7.5, w/w). After hydrolysis at $h = 8$, the sol-gel product together with added methanol was finally high-temperature supercritically dried in a batch operation. The BET surface area and pore volume of the uncalcined material amounted to 651 $m^2\ g^{-1}$ and 2.78 $cm^3\ g^{-1}$, respectively. The textural characteristics of the mixed aerogel were higher than those of the corresponding unitary oxide aerogels.

With regard to alumina–titania with 90 wt% Al_2O_3, Hoang-Van et al. [80] reported on the preparation of binary alumina-based oxide–oxide aerogels via either co-hydrolysis or a two-step procedure. In the co-hydrolysis procedure, aluminium(III) tri-sec-butoxide and titanium(IV) tetraisopropoxide in isopropanol were simultaneously hydrolyzed at a hydrolysis level of 4 and the resulting alcogels were supercritically dried above the appropriate critical conditions. For the two-step procedure, the hydrolysis of titanium(IV) tetraisopropoxide was followed by the introduction of pre-prepared alumina aerogel. The solvent was again removed by high-temperature supercritical drying. The uncalcined alumina–titania aerogel prepared by co-hydrolysis was X-ray amorphous and exhibited a much higher BET surface area (615 $m^2\ g^{-1}$) than those of the corresponding single aerogels (100 $m^2\ g^{-1}$, titania; 490 $m^2\ g^{-1}$, alumina) and binary aerogel synthesized by the two-step procedure (510 $m^2\ g^{-1}$). In contrast to co-hydrolysis, the two-step procedure led to the formation of anatase and boehmite, indicative of the absence of thorough interaction between alumina and titania.

For completeness, Ayen and Iacobucci [50] prepared a number of binary and ternary aerogels via an alkoxide-based sol-gel process followed by semicontinuous extraction with supercritical CO_2. As-received alumina–titania, silica–yttria–titania, and alumina–yttria–titania possessed compositions of 50/50, 5/5/90 and 82/3/15 wt%, BET surface areas of 750, 700 and 490 $m^2\ g^{-1}$, and pore volumes of 1.2, 1.3, and 0.6 $cm^3\ g^{-1}$, respectively. For all materials EDX mapping at high magnification indicated homogeneously mixed oxides.

4. Metal–titania aerogels

4.1. Rh, Ni, or Pt containing silica–titania aerogels

The use of silica–titania aerogels as dispersion matrix for active metals (Rh, Ni, Pt) was exploited in a series of studies [71,81,82]. The metals were deposited by impregnation of aerogels or added during the wet-chemical stage of sol-gel processing.

Silica–titania aerogel-supports with up to 10 mol% TiO_2 were prepared either by mixing an ethanolic solution of tetraethoxysilicon(IV), H_2O, and HCl ($h = 4$) with butanolic tetrabutoxytitanium(IV) modified by acetic acid (acetic acid/tetrabutoxytitanium(IV) = 5.5) or via prehydrolysis of the tetraethoxysilicon(IV)-containing solution under ultrasound and subsequent addition of the modified titania precursor (sonogel). The as-received gels were dried by solvent exchange with isoamyl acetate and further low-temperature supercritical drying with CO_2 (315 K). After calcination at 773 K, the silica–titania mixed oxides were impregnated with a solution of the noble metal precursor. An alternative introduction of the metallic component was the addition of Rh or Ni precursors during the sol-gel process (one-step method). In these cases, aqueous solutions of the metal pre-

cursors were used for the ultrasonically assisted prehydrolysis of tetraethoxysilicon(IV), which was again followed by the addition of the modified titania precursor. In general, the metal loadings amounted to 2.5 wt% for Rh and Ni and 0.9 wt% for Pt.

Studies on the catalytic activity of Rh-containing silica–titania with 10 mol% TiO_2 in benzene hydrogenation [81] at 303 K showed that the catalysts synthesized by impregnation afforded high dispersions of Rh and an increase of the catalytic activity in parallel with the pretreatment temperature ($\leq$ 773 K) in flowing hydrogen. The samples prepared via addition of Rh in the sol-gel process, however, resulted in poor metallic dispersion as well as activity, and revealed the capability of uptaking large amounts of hydrogen via spillover. It is noteworthy that both patterns of behavior largely differed from that of a catalyst prepared by impregnation of commercial silica with a solution of tetrabutoxytitanium(IV) in hexane [10 mol% TiO_2 relative to (SiO_2 + TiO_2)] and subsequent deposition of Rh.

As concerns the hydrogenolysis of n-butane with Rh [71,82], Ni [82], or Pt [71], the percentage of titania (0–10 mol% TiO_2), the method used for the introduction of the metal (see above), and the nature of the metal itself (Rh, Ni, Pt) affected both activity and selectivity. The increase of the titania content in Rh on silica–titania catalysts from 0 to 10 mol% TiO_2 yielded a significant rise in hydrogenolysis activity with selectivities to ethane higher than 80%. Moreover, the use of sonogel supports led to superior activity compared to the silica–titania support prepared without ultrasound-prehydrolysis (see Section 3.2.). The one-step Rh catalysts exerted again a different behavior; they did not direct the reaction towards a definite product. With regard to Ni supported on sonogel supports [82], the dispersions were lower than those of the corresponding Rh catalysts and high selectivities to the breakdown of C–C terminal bonds were observed. The one-step synthesis led to much lower dispersions and thus less selective hydrogenolysis activity only above 650 K.

4.2. Pt–titania and Pd–titania aerogels

Instead of mixing titanium and noble metal components at the beginning of the sol-gel process, titania gels were first prepared and subsequently redispersed in order to return to the "primary" structure of the titania matrix [83,84]. (For the preparative concept, see Section 3.1.) This procedure provided the advantage of homogeneously dispersing the noble metal precursor in the sol-gel product. Another beneficial aspect arose from the use of preformed "colloidally" dispersed titania, which helps to prevent the occlusion of precious noble metal particles. High-temperature Pt–titania [83] and Pd–titania [84] aerogels with meso- to macroporosity and in situ formed uniformly distributed metallic particles possessed high accessibility of the internal surface for bulky reactants in liquid-phase hydrogenation and stability of both titania matrix and metal particles.

This advantageous aspect of the marked porosity with large accessibility emerged from a comparison of the activities in liquid-phase hydrogenation of *trans*-stilbene (303 K) and benzophenone (343 K) over a Pt–titania high-temperature aerogel calcined in air at 673 K and a commercial Pt-on-alumina catalyst [83], illustrated in Fig. 8. The Pt–titania aerogel possessed a meso- to macroporous pore size distribution with a maximum at ca. 50 nm, the commercial Pt-on-alumina catalyst, a micro- to mesoporous one, with a maximum at ca. 4 nm. Wide pores made the large "internal" surface area highly accessible for bulky reagents, minimizing effects of pore diffusion control and consequently yielding a high effectiveness factor. Both *trans*-stilbene and benzophenone are bulky molecules of 0.5 × 1.1 and 0.5 × 1.0 nm, respectively. Considering the similar dispersions of both catalysts, the superior hydrogenation activity of the Pt–titania aerogel was likely due

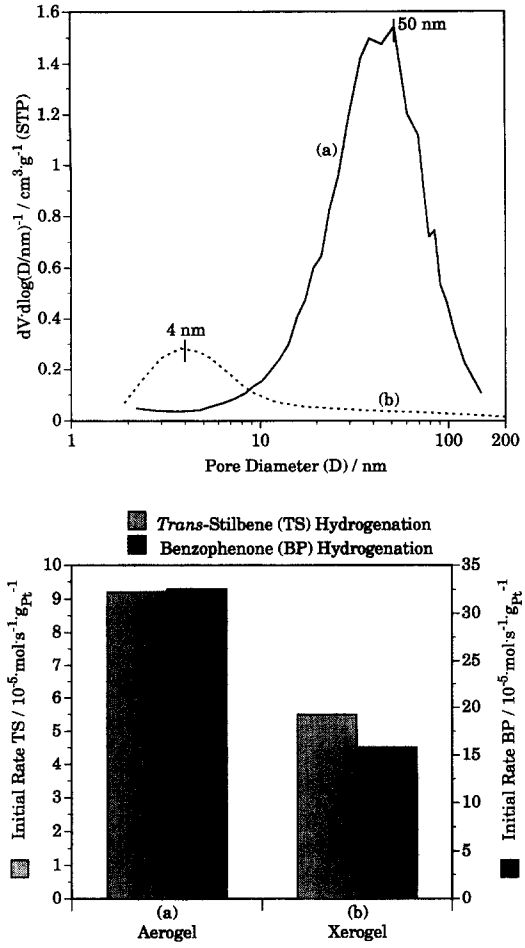

Fig. 8. Influence of the accessibility of internal surface, illustrated by the differential pore size distributions derived from nitrogen physisorption at 77 K (STP; 273.15 K, 1 atm) (top), on the initial rates for liquid-phase hydrogenation of *trans*-stilbene and benzophenone (bottom). (a) Pt–titania high-temperature aerogel calcined in air at 673 K; (b) commercial Pt-on-alumina xerogel catalyst (Engelhard 7004). Both with 5 wt% Pt and similar metal dispersions of ca. 0.3. Data were taken from Ref. [83].

to its higher accessibility compared to the Pt-on-alumina xerogel. This behavior was supported by the dependence of the hydrogenation activity of the commercial catalyst on the particle size above ca. 50 μm, indicative of mass transfer limitation. As to the aerogel, the hydrogenation activities were independent of the particle size up to at least 500 μm. Moreover, the pore structure was virtually preserved in solution, as inspection of the textural properties after catalytic use and conventional redrying indicated.

Table 3 shows the catalytic data for 4-methylbenzaldehyde hydrogenation over Pd–titania aerogel catalysts with 2 and 5 wt% Pd (Pd2PAc, Pd5PAc), both calcined in air at 673 K [84]. Data for a low acidity and high acidity 0.5 wt% titania-supported Pd catalyst are included for comparison. These catalysts were prepared by impregnation of titania extrudates (phase ratio of anatase/rutile, 3:1), subsequent calcination in air, and reduction under a H_2–N_2 atmosphere. The tests were carried out using the same Pd/reactant ratio. The results indicate that the aerogel catalysts possessed much higher hydrogenation activity (Table 3). Almost full conversion to 4-methylbenzyl alcohol could be achieved in 0.5–1 h at considerably lower temperature and hydrogen pressure. The hydroxymethyl group of the benzyl alcohol derivative was subsequently converted to the corresponding methyl group. Note that the reduction of aromatic aldehydes on Pd is generally faster than the further reduction of the intermediate aromatic alcohols. Another interesting point was the negligible formation of ethyl 4-methylbenzyl ether after 4 h. The catalytic tests indicated that the aerogel catalysts were very active in the reduction of the carbonyl group in 4-methylbenzaldehyde to the corresponding hydroxyl group and in the hydrogenolysis of the C–O bond to form hydrocarbons, but ethyl 4-methylbenzyl ether formation was negligible due to the absence of strong acid sites.

Concerning the genesis of the metal constituent in metal–metal oxide sol-gel catalysts, the drying method applied is one of the decisive factors influencing the oxidation state, dispersion, and accessibility of the metallic constituent. In terms of the oxidation state, high-temperature supercritical drying readily forces the in situ reduction of metal ions, and the as-received metal–metal oxide aerogels often reveal high catalytic activity without any subsequent thermal activation. This reduction is supported by X-ray photoelectron spectroscopy [85]

Table 3
Catalytic activity of palladium-containing titania catalysts in the liquid-phase hydrogenation of 4-methylbenzaldehyde (A) to 4-methylbenzyl alcohol (B), p-xylene (C), ethyl 4-methylbenzyl ether (D)

Catalyst	Time (h)	Temp. (K)	Pressure (MPa) [a]	Product composition (%)			
				A	B	C	D
Pd2PAc (calcined in air at 673 K)	1	333	0.05	3	80	17	0
	4	333	0.05	2	12	86	0
Pd5PAc (calcined in air at 673 K)	0.5	333	0.05	3	95	2	0
	4	333	0.05	3	18	79	0
0.5 wt% Pd/TiO_2 (Pd 6)	4	423	1	5	15	71	7
0.5 wt% Pd/TiO_2 (Pd 1C)	4	423	1	26	0	0	73

Note. Data taken from Ref. [84].
[a] Hydrogen partial pressure.

and additionally justified on the basis of investigations concerning the preparation of Pt and Pd sols in refluxing methanol at 338 K and ambient pressure [86,87]. For Pt, the particles were shown to be metallic by extended X-ray absorption fine structure analysis and high-resolution transmission electron microscopy [87]. Note that temperatures > ca. 510 K and alcoholic pressures of ca. 10 MPa are applied during high-temperature supercritical drying. In contrast to high-temperature aerogels, low-temperature aerogels and xerogels have to be thermally activated after drying and prior to catalytic use, in order to establish the metallic state. Besides the different drying methods, the formation of the metallic component is determined by the balances between the processes of nucleation, autocatalytic reductive growth, homo- and heterocoagulation in the presence of the solvent, and by the extent of sintering once the solvent is removed. These processes are in turn affected by such factors as the nature of the solvent as well as metal precursor, pH, concentrations and concentration heterogeneities, presence of stabilizers, extent of binding of the precursor to the support, surface charge, mobility of the nascent metal particles, drying conditions, and last but not least the thermal treatment of the as-received solid. Fig. 9, extracted from Refs. [83,84], represents the essential dependence of the metal dispersions on both the metal (Pt or Pd) and the metal precursor. As discussed above, the accessibility of the active component may be reduced by organic contaminants, persisting in the dry sol-gel product; the amount strongly depends on the drying method applied. In the case of high-temperature supercritical drying, another important factor has to be taken into account. The high temperature coupled with enhanced solvent reactivity leads to restructuring phenomena, which are likely to cause occlusion of the metal particles by partial embedding and coverage with reprecipitated oxide species from the matrix. The processes concerned are dissolution, reprecipitation, esterification, and syneresis (see Section 4.1.).

4.3. Polymer-stabilized Pt colloids supported on titania aerogels

The metallic component can be introduced by either impregnation, equilibrium-deposition–filtration, ion exchange, and other immobilization methods or the direct addition of the metal precursor during the wet-chemical sol-gel process.

An alternative route via heterogenization (immobilization) of preformed colloids was reported by Duff et al. [88]. As to the preparation of the metal sol (colloidal dispersion) in methanol, a methanolic solution of chloroplatinic acid was added to polyvinylpyrrolidone dissolved in methanol. This clear solution was heated to boiling under continuous nitrogen flow

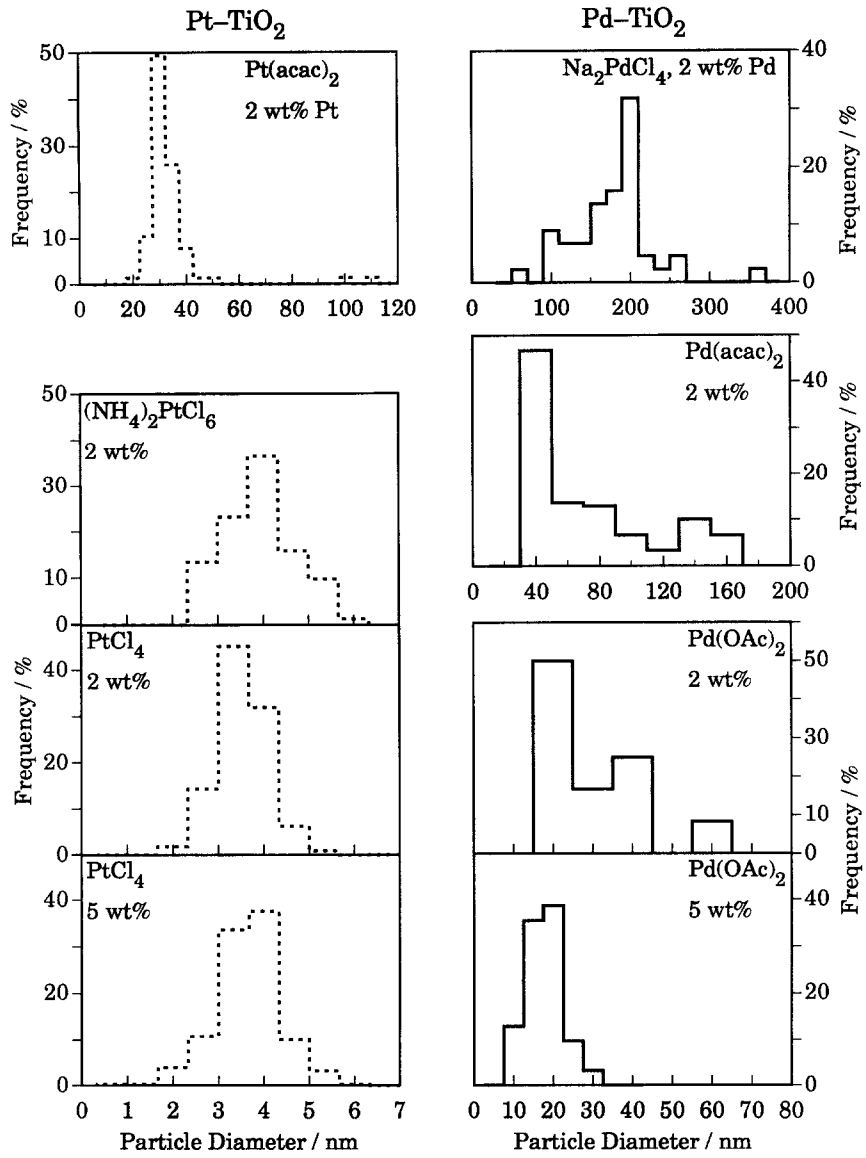

Fig. 9. Metal particle size distributions, derived from transmission electron microscopy, of untreated Pt–titania (left side, ---) [83] and Pd–titania (right side, —) [84] aerogels. The chemical formulas represent the noble metal precursor used.

and boiled under reflux. During boiling the color of the solution changed spontaneously to dark brown as the platinum colloids formed. To prepare a heterogeneous catalyst, a volume of the as-received sol was mixed with a methanolic suspension of a high-surface-area titania aerogel (anatase, ca. 200 $m^2\ g^{-1}$; $V\varnothing$ from Ref. [59]) which had been exposed to low-energy ultrasonic irradiation to improve the dispersion of the powder in the solvent. The supported catalyst was filtered and washed with methanol. The amounts were chosen to give a 2% Pt by weight catalyst. The filtrates were in every case colorless, indicating (near-) quantitative adhesion of platinum particles to the support as well as the absence of significant quantities of unreduced, unadsorbed ions. The loading was independently confirmed by ICP-AES. The unsupported

Pt-sol exhibited high activity for the hydrogenation of *trans*-stilbene and methylcinnamate. Although polyvinylpyrrolidone restricted access to the surface, it is extremely well solvated in methanol. It will thus be extended in conformation forming a solvent-rich surface layer allowing diffusion of reactant molecules to the metal surface. Uncalcined, supported Pt-sol catalysts generally possessed lower activity, the support further restricted access of reactant to the Pt surface. Upon calcination at 573 K, however, the accessibility of the Pt surface for the organic reactants was enhanced through oxidative removal of polyvinylpyrrolidone from the particle surfaces. In the case of *trans*-stilbene hydrogenation, the deactivation of the most active catalysts probably occurred by virtue of alkene polymerization in the presence of oxidized but not fully removed organic residues and/or acidic supports.

The striking similarity of the particle size distributions of Pt-sol on titania-aerogel [88] and Pt–titania aerogel prepared by a one-step method [83] allows an interesting comparison, which is depicted in Fig. 10. Both contained 2 wt% Pt derived from chloroplatinum precursors. The titania support for the Pt-sol was synthesized similarly to the titania matrix of the binary Pt–titania aerogel. In both cases the crystalline fractions of titania consisted of well developed anatase crystallites and the textural properties were almost identical; methanol was the solvent in both cases. As regards the Pt–titania aerogel [83], the metal particles were formed in situ from $PtCl_4$ dissolved in MeOH–H_2O together with the titania matrix during supercritical drying. The catalytic activities for the hydrogenation of *trans*-stilbene under almost identical conditions were, however, markedly different (Fig. 10). The supported colloid sample was 3–4 times more active after calcination than the one-step sample. The Pt–titania aerogel, prepared without polyvinylpyrrolidone present, did not show the marked rise in catalytic activity after oxidative heat-treatment at 573 K that the immobilized Pt-sol samples exhibited. This difference in the activities probably reflected the different accessibility of the platinum particles for medium-large reactants in each case. With the sol method, the metal particles at coverage lower than saturation will preferentially stick to well exposed areas of support and can not in any case penetrate into the smaller pores. A high proportion of the metal surface is thus accessible for the reactants. By contrast in the case of the one-step preparations the metal particles are very homogeneously distributed and partially occluded in a highly porous titania-aerogel matrix [83]. Although resulting in a lower specific activity, this aspect favors both

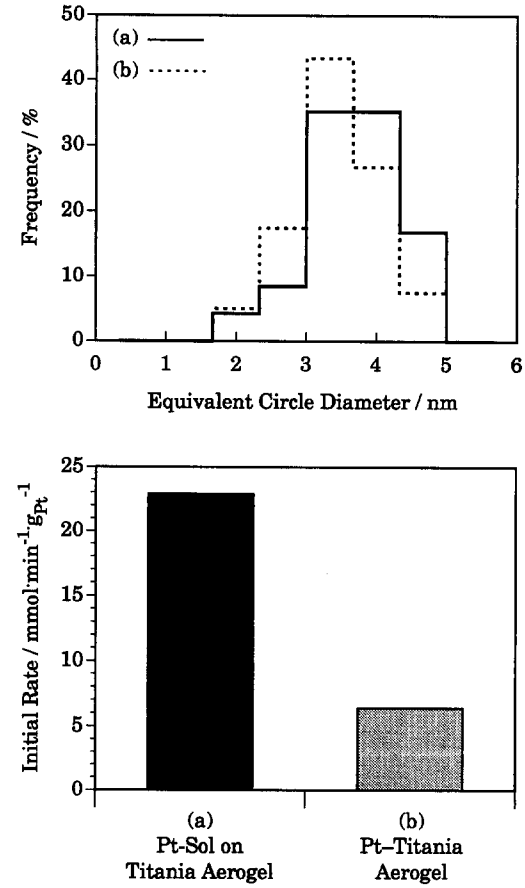

Fig. 10. Comparison of Pt-sol immobilized on a titania aerogel (a) with a binary Pt–titania aerogel prepared by a one-step sol-gel–aerogel route (b). Both catalysts were calcined at 573 K and contained 2 wt% Pt. Top: metal particle size distributions; bottom: initial rates for the hydrogenation of *trans*-stilbene at ambient hydrogen pressure. Data were taken from Ref. [88].

thermal and abrasive stability for the one-step sol-gel systems.

5. Conclusions

The sol-gel technology eventually in combination with the different methods of supercritical drying offers valuable means for the preparation of titania-based catalytic materials with marked uniformity and exceptional properties. The sol-gel–aerogel preparation of titania has proved to be an interesting alternative. Morphological, structural, and chemical properties that largely differ from the properties of conventionally prepared titania-based solids are porosity, surface area, uniformity or homogeneity, novel redox and/or acid–base functionalities, and thermal stability.

Although the sol-gel method, both itself and in combination with supercritical drying, offers a potent means for the controlled preparation of solids with interesting textural, structural, and chemical properties, the technical application of sol-gel catalysts is hampered. The key problems are the rather high costs and, concerning the aerogels in particular, the manifold difficulties encountered in transferring them into an applicable form (heat-, mass-, and impulse-transfer restrictions) as well as the technical risks associated with supercritical drying (high-pressure and optionally high-temperature technologies). As to the costs, promising means are the use of inorganic salts, followed by exchange of the aqueous pore liquid for organic solvents, and the application of solid aggregates consisting of colloidal subunits. Moreover, the subcritical preparation of aerogel-like materials via freeze-drying, drying control chemical additives, pore size control, binders, exchange of the pore liquid for solvents with low surface tension, and surface modification with surfactants or chemically bound compounds offers potent alternatives for the high-pressure aerogel-technologies. Concerning heat-, mass-, and impulse-transfer constraints, noteworthy expedients are the fixation of aerogels as well as aerogel-like materials on open-form supports (honeycombs, foams, pellets, etc.), the extrusion of pre-synthesized aerogels as well as aerogel-like materials, and the synthesis of composite materials.

References

[1] T.A. Egerton, in D. Bloor, R.J. Brook, M.C. Flemings and S. Mahajan (Eds.), Encyclopedia of Advanced Materials, Vol. 4, Pergamon, Oxford, 1994, p. 2880.
[2] G.C. Bond and S.F. Fischer, Appl. Catal., 71 (1991) 1.
[3] H. Knözinger and E. Taglauer, Catalysis (London), 10 (1993) 1.
[4] S.J. Tauster, S.C. Fung and R.L. Garten, J. Am. Chem. Soc., 100 (1978) 170; S.J. Tauster and S.C. Fung, J. Catal., 55 (1978) 29.
[5] S.J. Tauster, S.C. Fung, R.T.K. Baker and J.A. Horseley, Science, 211 (1981) 1121; S.J. Tauster, Acc. Chem. Res., 20 (1987) 389.
[6] G.L. Haller and D.E. Resasco, Adv. Catal., 36 (1989) 173.
[7] B. Sen and M.A. Vannice, J. Catal., 113 (1988) 52.
[8] M.A. Vannice and B. Sen, J. Catal., 115 (1989) 65.
[9] C.G. Raab and J.A. Lercher, Catal. Lett., 18 (1993) 99.
[10] M. Guisnet, J. Barbier, J. Barrault, C. Bouchoule, D. Duprez, G. Pérot and C. Montassier, Stud. Surf. Sci. Catal., 78 (1993).
[11] N. Serpone and E. Pelizetti (Eds.), Photocatalysis – Fundamentals and Applications, Wiley, New York, 1989.
[12] C.J. Brinker and G.W. Scherer, Sol-gel Science – the Physics and Chemistry of Sol-gel Processing, Academic Press, San Diego, 1990.
[13] J. Livage, M. Henry and C. Sanchez, Prog. Solid State Chem., 88 (1988) 259.
[14] D.C. Bradley, R.C. Mehrotra and D.P. Gaur, Metal Alkoxides, Academic Press, London, 1978.
[15] R.C. Mehrotra, D.P. Gaur and R. Bohra, Metal β-diketonates and Allied Derivatives, Academic Press, London, 1978.
[16] R.C. Mehrotra and R. Bohra, Metal Carboxylates, Academic Press, London, 1983.
[17] M. Schneider and A. Baiker, Catal. Rev.–Sci. Eng., 37 (1995) 515.
[18] J. Fricke and A. Emmerling, Struct. Bonding, 77 (1992) 37.
[19] G.M. Pajonk, Appl. Catal., 72 (1991) 217.
[20] M.A. Cauqui and J.M. Rodriguez-Izquierdo, J. Non-Cryst. Solids, 147&148 (1992) 724.
[21] D.A. Ward and E.I. Ko, Ind. Eng. Chem. Res., 34 (1995) 421.
[22] Thermodynamics Research Center, The Texas A and M University System, TRC Thermodynamic Tables, College Station, TX, USA.
[23] C.J. Brinker, R. Sehgal, S.L. Hietala, R. Deshpande, D.M. Smith, D. Loy and C.S. Ashley., J. Membr. Sci., 94 (1994) 85.
[24] R.W. Pekala, C.T. Alviso, S.S. Hulsey and F.-M. Kong, MD (Am. Soc. Mech. Eng.), 38 (1992) 129.

[25] S.S. Prakash, C.J. Brinker, A.J. Hurd and S.M. Rao, Nature, 374 (1995) 439.
[26] C. Liu and S. Komarneni, Mater. Res. Soc. Symp. Proc., 371 (1995) 217.
[27] R. Kozlowski, R.F. Pettifer and J.M. Thomas, J. Phys. Chem., 87 (1983) 5172.
[28] C. Lijzenga, V.T. Zaspalis, C.D. Ransijn, K.P. Kumar, K. Keizer and A.J. Burggraf, Key Eng. Mater., 61&62 (1991) 379.
[29] E.A. Barringer and H.K. Bowen, Langmuir, 1 (1985) 414.
[30] M.A. Anderson and Q. Xu, Wisconsin Alumni Research Foundation, WO Patent No. 92/19 369 (1992).
[31] A. Moini, Mobil Oil Corporation, US Patent No. 5162283 (1992).
[32] I.A. Montoya, T. Viveros, J.M. Dominguez, L.A. Canales and I. Schifter, Catal. Lett., 15 (1992) 207.
[33] B.E. Yoldas, J. Mater. Sci., 21 (1986) 1087.
[34] A. Léaustic and R.E. Riman, J. Non-Cryst. Solids, 135 (1991) 259.
[35] R.J.P. Corriu, D. Leclercq, P. Lefèvre, P.H. Mutin and A. Vioux, J. Mater. Chem., 2 (1992) 673.
[36] C. Roger and M.J. Hampden-Smith, J. Mater. Chem., 2 (1992) 1111.
[37] M.A. Vicarini, G.A. Nicolaon and S.J. Teichner, Bull. Soc. Chim. Fr., 1970, p. 1651.
[38] S.J. Teichner, G.A. Nicolaon, M.A. Vicarini and G.E.E. Gardes, Adv. Colloid Interface Sci., 5 (1976) 245.
[39] M. Formenti, F. Juillet, P. Meriaudeau and S.J. Teichner, Bull. Soc. Chim. Fr., 1972, p. 69.
[40] C. Sanchez, J. Livage, M. Henry and F. Babonneau, J. Non-Cryst. Solids, 100 (1988) 65.
[41] M. Schneider, Titania Based Aerogel Catalysts, Dissertation ETH No. 10685, Swiss Federal Institute of Technology, Zürich, 1994.
[42] M. Schneider and A. Baiker, J. Mater. Chem., 2 (1992) 587.
[43] K. Chhor, J.F. Bocquet and C. Pommier, Mater. Chem. Phys., 32 (1992) 249.
[44] C. Pommier, K. Chhor and J.F. Bocquet, Silic. Ind., 59 (1994) 141.
[45] J.F. Bocquet, K. Chhor and C. Pommier, Surf. Coat. Technol., 70 (1994) 73.
[46] C.H. Shin, G. Bugli and G. Djega-Mariadassou, J. Solid State Chem., 95 (1991) 145.
[47] N.R. Hunter, H.D. Gesser, L.A. Morton, P.S. Yarlagadda and D.P.C. Fung, Prepr. Am. Chem. Soc., Div. Pet. Chem., 32 (1987) 779.
[48] L.W. Hrubesh and R.W. Pekala, J. Mater. Res., 9 (1994) 731.
[49] S.D. Ramamurthi and M. Ramamurthi, Battelle Memorial Institue, WO Patent No. 93/06 044 (1993); S. Ramamurthi and M. Ramamurthi, Battelle Memorial Institute, US Patent No. 5306555 (1994).
[50] R.J. Ayen and P.A. Iacobucci, Rev. Chem. Eng., 5 (1988) 157.
[51] L.K. Campbell, B.K. Na and E.I. Ko, Chem. Mater., 4 (1992) 1329.
[52] C.J. Brodsky and E.I. Ko, J. Mater. Chem., 4 (1994) 651.
[53] D.C.M. Dutoit, M. Schneider and A. Baiker, J. Porous Mater., 1 (1995) 165.
[54] G. Dagan and M. Tomkiewicz, J. Phys. Chem., 97 (1993) 12651; G. Dagan and M. Tomkiewicz, J. Non-Cryst. Solids, 175 (1994) 294.
[55] Z. Zhu and M. Tomkiewicz, Mater. Res. Soc. Symp. Proc., 346 (1994) 751.
[56] B.B. Mandelbrot, The Fractal Geometry of Nature, Freeman, San Francisco, 1982; D. Avnir, The Fractal Approach to Heterogeneous Chemistry – Surfaces, Colloids, Polymers, Wiley, New York, 1989.
[57] J. Engweiler and A. Baiker, Appl. Catal. A, 120 (1994) 187.
[58] A. Baiker, B. Handy, J. Nickl, M. Schraml and A. Wokaun, Catal. Lett., 14 (1992) 89.
[59] M. Schneider, M. Maciejewski, S. Tschudin, A. Wokaun and A. Baiker, J. Catal., 149 (1994) 326.
[60] U. Scharf, M. Schneider, A. Baiker and A. Wokaun, J. Catal., 149 (1994) 344.
[61] H. Schneider, S. Tschudin, M. Schneider, A. Wokaun and A. Baiker, J. Catal., 147 (1994) 5.
[62] M. Schneider, U. Scharf, A. Wokaun and A. Baiker, J. Catal., 150 (1994) 284.
[63] D.C.M. Dutoit, M. Schneider and A. Baiker, J. Catal., 153 (1995) 165, and further references concerning silica–titania mixed oxides therein.
[64] R. Hutter, T. Mallat and A. Baiker, J. Catal., 153 (1995) 177.
[65] G. Cogliati, Enichem S.p.A., European Patent No. 0454239 (1991).
[66] G. Cogliati, M. Guglielmi, T.M. Che and T.J. Clark, Mater. Res. Soc. Symp. Proc., 180 (1990) 329.
[67] G. Cogliati and G. Bezzi, Enichem S.p.A., European Patent No. 0383378 (1990).
[68] M. Beghi, P. Chiurlo, L. Costa, M. Palladino and M.F. Pirini, J. Non-Cryst. Solids, 145 (1992) 175.
[69] M. Beghi, P. Chiurlo, G. Cogliati, L. Costa, M. Palladino and M.F. Pirini, Eur. Mater. Res. Soc. Monogr., 5 (1992) 283.
[70] J.J. Calvino, M.A. Cauqui, G. Cifredo, J.A. Perez and J.M. Rodriguez-Izquierdo, Mater. Res. Soc. Symp. Proc., 346 (1994) 685.
[71] S. Bernal, J.J. Calvino, M.A. Cauqui, J.M. Rodriguez-Izquierdo and H. Vidal, Stud. Surf. Sci. Catal., 91 (1995) 461.
[72] J.J. Calvino, M.A. Cauqui, G. Cifredo, L. Esquivias, J.A. Perez, M. Ramirez del Solar and J.M. Rodriguez-Izquierdo, J. Mater. Sci., 28 (1993) 2191.
[73] M. Ramirez del Solar and L. Esquivias, J. Sol–gel Sci. Technol., 3 (1994) 41.
[74] J.B. Miller, S.T. Johnston and E.I. Ko, J. Catal., 150 (1994) 311.
[75] P.A. Iacobucci, C.-P. Cheng and E.N. Walsh, Stauffer Chemical Company, European Patent No. 0186149 (1985).
[76] C.-P. Cheng and P.A. Iacobucci, Stauffer Chemical Company, European Patent No. 0149816 (1984).
[77] B.G. Pazol and A.C. DeFranzo, Proc. SPIE Int. Soc. Opt. Eng., 2018 (1994) 167.
[78] J.G. Weissman, E.I. Ko and S. Kaytal, Appl. Catal. A, 94 (1993) 45.
[79] S.M. Maurer, D. Ng and E.I. Ko, Catal. Today, 16 (1993) 319.
[80] C. Hoang-Van, R. Harivololona and B. Pommier, Stud. Surf. Sci. Catal., 91 (1995) 435.

[81] M.A. Cauqui, J.J. Calvino, G. Cifredo, L. Esquivias and J.M. Rodriguez-Izquierdo, J. Non-Cryst. Solids, 147 and 148 (1992) 758.
[82] J.J. Calvino, M.A. Cauqui, J.M. Gatica, J.M. Rodriguez-Izquierdo and H. Vidal, J. Sol-Gel Sci. Technol., 2 (1994) 831.
[83] M. Schneider, D.G. Duff, T. Mallat, M. Wildberger and A. Baiker, J. Catal., 147 (1994) 500.
[84] M. Schneider, M. Wildberger, M. Maciejewski, D.G. Duff, T. Mallat and A. Baiker, J. Catal., 148 (1994) 625.
[85] J.N. Armor, E.J. Carlson and P.M. Zambri, Appl. Catal., 19 (1985) 339.
[86] H. Hirai, Y. Nakao and N. Toshima, J. Macromol. Sci. Chem. A, 13 (1979) 727.
[87] D.G.Duff, P.P. Edwards, J. Evans, J.T. Gauntlett, D.A. Jefferson, B.F.G. Johnson, A.I. Kirkland and D.J. Smith, Angew. Chem. Int. Ed. Engl., 28 (1989) 590.
[88] D.G. Duff, T. Mallat, M. Schneider and A. Baiker, Appl. Catal. A, 133 (1995) 133.